IEEE Access
Multidisciplinary | Rapid Review | Open Access Journal

Received 29 March 2023, accepted 8 April 2023, date of publication 13 April 2023, date of current version 20 April 2023.

Digital Object Identifier 10.1109/ACCESS.2023.3266813

RESEARCH ARTICLE

Automated Construction of Mesoscopic Railway Infrastructure Models Supporting Station Throat Capacity Assessment

PETR VESELÝ[1], ANTONÍN KAVIČKA[1], AND PAVEL KRÝŽE[2]
[1]Faculty of Electrical Engineering and Informatics, University of Pardubice, 532 10 Pardubice, Czech Republic
[2]Správa železnic, s. o. (Railway Infrastructure Administration, State Organization), 110 00 Prague, Czech Republic

Corresponding author: Antonín Kavička (antonin.kavicka@upce.cz)

This work was supported by the European Regional Development Fund (ERDF)/European Structural Fund (ESF) within the Project "Cooperation in Applied Research Between the University of Pardubice and companies, in the field of positioning, detection and simulation technology for transport systems (PosiTrans)" under Grant CZ.02.1.01/0.0/0.0/17_049/0008394.

ABSTRACT Assessment of the traffic capacity of a rail infrastructure involved within railway stations is one of the basic components of the rail transport planning process. An important part of the rail infrastructure in the stations is station throat, which typically comprises many switches and track crossings. Station throat acts as operating bottleneck that frequently has the largest impact on the station's traffic capacity. The capacity of a station throat is often conveniently assessed based on the use of mesoscopic computer simulation. This requires (among other things) a suitable submodel of the throat infrastructure to be set up. This article presents innovative algorithms for the automated creation of mesoscopic target model of station throat based on consecutive transformations of an initial (intuitive) microscopic model. Compared to the hitherto used manual process, the automated procedure accelerates the construction of the target station throat model and eliminates its structural errors. The applied research method is based both on the original design of the target mathematical model graph (a vertex-weighted directed graph) for the representation of the station throat infrastructure and on the design and verification of innovative graph algorithms that perform multiple aggregation transformations of this model in order to perform its maximum admissible topological simplification. The results of the research conducted have helped to enhance and efficiently use the station throat capacity assessment methodology. The use of the algorithms is demonstrated in a case study concerning station throats within a minor railway station in the Czech Republic.

INDEX TERMS Rail infrastructure models, rail traffic simulation, capacity assessment, station throat.

I. INTRODUCTION

To ensure the efficient operation of the rail transport system, railway companies all over the world use traffic planning procedures encompassing different time horizons. *Strategic* (*long-term*) *planning* focuses on planning and assessing changes within the rail infrastructure whose topology will affect rail transport in the long run. *Medium-term* (*tactical*) *planning* is typically focused on setting up the *timetables* and assessing the traffic feasibility. *Short-term* (*operative*) *planning* and *control* address problems existing within the current rail transport (e.g., such as assigning alternative platform tracks to trains whose arrival is delayed etc.).

The topic described in this article is related to the rail infrastructure capacity assessment with a focus on *station throat*, which normally interconnects *station tracks* and *line tracks* (Fig. 1). Station throat constitutes a continuous zone within the railway yard, consisting of many *switches* and, as the case may be, *track crossings*. Station throats largely constitute operating bottlenecks with impacts on the rail yard capacity. This problem can be addressed within strategic planning or tactical planning. If the design of new or rebuilt

The associate editor coordinating the review of this manuscript and approving it for publication was Jesus Felez.

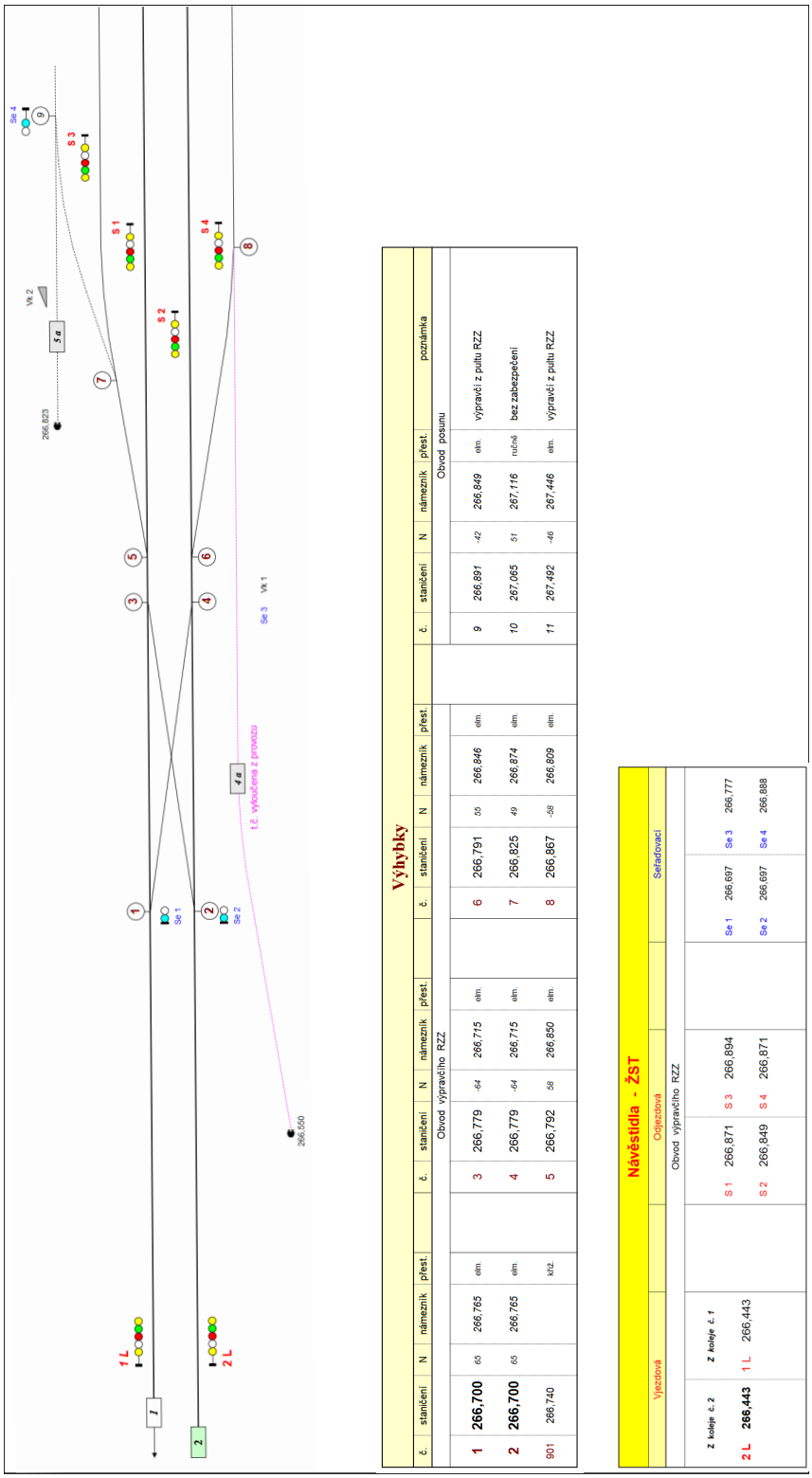

FIGURE 1. The fragment of an illustrative schematic track layout.

(expanded) station throat is assessed from the rail traffic aspect, this process falls within strategic planning. If existing station throat is assessed with respect to a specific future traffic variant, e.g., in the context of setting up a new timetable, the investigation is made for tactical planning purposes.

The station throat capacity can be examined by using different methods/procedures making use, e.g., of analytical calculations [1], [2] or computer simulation [3], [4]. The present article describes an original innovation of the *SepSim-Z* methodology (*Separate Simulation of rail traffic*

on station throat), which is used in the Czech Republic for examining the traffic characteristics of the station throats based on (mesoscopic) computer simulation. This separate simulation examines rail traffic within the specific station throat analyzed while disregarding traffic on the remaining segments of the rail yard. The *w* indicator – *waiting times of trains in traffic* – is conventionally used when assessing the station throat capacity. This indicator quantifies the waiting time (in minutes) of each train during the (simulated) rail traffic. Waiting is a result of what is referred to as *conflicts* on the station throat: a conflict is a situation where a train cannot enter the station throat because the area is currently used by another train (or a shunting process is underway). Once the conflict is resolved, the train ceases to wait. The *SepSim-Z* methodology (described in Directive *SM124* [5]) specifies *limit values* for the waiting times of trains in traffic. Two characteristic waiting time values are used: the *optimum* waiting time w_{opt} and the *critical* waiting time w_{crit}. The limit values can be used for a comparison with the statistically processed train waiting times obtained from the separate simulation (mirroring the traffic on the specific station throat). The result of this comparison is used to assess the station throat capacity.

An important role in the *SepSim-Z* methodology is played by a computer simulator to perform stochastic mesoscopic simulation of rail traffic on a specific station throat. The simulation requires, among other things, a suitable model of the throat infrastructure on which the adequately specified rail traffic takes place. So far, the target mesoscopic submodels of the station throats have been set up manually by using various transformations of the initial intuitive microscopic throat model. This manual approach, however, can be frequently a source of structural errors that are not easy to detect.

A. MOTIVATION TO ENHANCE THE METHODOLOGY

Within the frame of the above mentioned *SepSim-Z* methodology, manual procedures have been used in practice so far for the creation of mesoscopic models of the station throat rail infrastructure. The construction of these models was relatively time consuming and there was no effective support for eliminating potential design errors in these models. From this perspective, there was a strong motivation to enhance the relevant part of this methodology. Thus, the main purpose of conducting the relevant R&D was to design, develop and verify innovative algorithms for the automated construction of target station throat models at the mesoscopic level of abstraction. The above research was important and much needed, as its results were used to enhance the quality and credibility of the *SepSim-Z* methodology. The content of the research itself was in particular the original design of the target mathematical model (a vertex-weighted directed graph) for the representation of the station throat infrastructure and the design and verification of innovative graph algorithms that perform multiple aggregation transformations of this model in order to reach its maximum abstraction rate (i.e., maximum admissible topological simplification). The algorithms and models are described in detail and their deployment is illustrated later in this article. The significance of the research carried out lies mainly in the fact that it contributed to the deployment of automated procedures in the part of the discussed methodology that could replace the manual approach.

B. RELATED LITERATURE

In terms of the context of the presented research results, a brief overview of the methods, approaches and methodologies used to investigate the capacities of differently sized segments of rail infrastructure is presented.

The capacity of the rail infrastructure can be assessed on different scales, which can be classified as follows:

- The *network-wide scale* is typically used when assessing the capacity (throughput) of a large rail network area [6], [7], [8], frequently encompassing one or more countries.
- The *regional scale* is used when assessing rail traffic within regions [9] or large railway junctions [10], where the various rail lines and railway stations are discerned.
- The *railway line scale* or *railway station scale* is typically used to examine the traffic capacity of a specific railway line [11] or a specific railway station [12].
- The *track throat scale* is used when separately assessing the capacity of station throat (both within a railway station and potentially also beyond) [13], [14].

The railway infrastructure capacity can be assessed (on any scale) by using analytical methods, simulation methods or combinations of both [15].

The following are examples of typical analytical methods used to assess the railway infrastructure capacity:

- *UIC 406 methodology* [2], covering both capacity assessment for railway lines [11], [16] and for railway stations [17], [18], [19] by using the compression method.
- The methodology used by *Deutsche Bahn AG* (*DB AG* – German Railways), which is primarily based on theoretical work done at the RWTH Aachen University [13], [20], [21]. The conditions for the use of the methodologies by *DB AG* are described in the directive *Richtlinie 405 – Fahrwegkapazität* [22].

Traffic simulations (aimed at railway infrastructure assessment) can apply the following levels of detail:

- *macroscopic* level of detail, particularly when establishing the characteristics of traffic flows i) for which it is normally not necessary to examine the various train entities in detail and (ii) where the use of a coarse model of the rail infrastructure is sufficient; this level of detail is typically used for operational examination of extensive railway networks,
- *microscopic* level of detail, which is typically used where one wishes to model in detail: (i) the run of each train (following a precise description of the motion dynamics), and (ii) the precise positions of each train on the infrastructure in defined time moments (and hence,

a very detailed rail infrastructure model is required); this level of detail may be applied in simulators mirroring the systems of different spatial extents (smaller regions, individual railway lines or stations, station throats),
- *mesoscopic* level of detail, which is typically used where (i) monitoring the individual trains is required, (ii) simplified modelling of the traffic is acceptable, and (iii) where the infrastructure models are less detailed than as used in microscopic simulators; this level of detail is typically used in simulators primarily focusing on the determination of the traffic capacity characteristics within systems reflecting differently extensive land areas (except for areas with large-scaled railway networks).

Software tools for *macroscopic rail traffic simulations* (such as NEMO [23], [24]) are typically used when assessing the capacity/throughput of large railway network areas in the context of strategic (long-term) planning. The operational indicators related to the determination of the network infrastructure capacity (and, where appropriate, additional indicator mirroring the robustness of the timetables) can be quite diverse. Their classification and practical uses are summarized, e.g., in [8] and [25].

Simulation tools for *microscopic rail traffic simulations* are designed for detailed monitoring of all movements of the rail vehicles by using very detailed rail infrastructure models. There are quite a number of tools in support of microscopic simulation, such as *Villon* [26], *RailSys* [27], *OpenTrack* [28] *PulSim* [29] and *SIMARAIL* [30]. Such tools are typically employed in such simulation studies in support of medium-term /tactical traffic planning as are focused on a very detailed evaluation of the traffic indicators in different traffic scenarios, aimed at the examination of different variants of the infrastructure as well as different variants of the timetables.

Simulators for *mesoscopic rail traffic simulation* are mainly used to examine train interactions and the related occurrences of conflicts [31], [32], [33]. Conflicts are linked to competition for track routes required for travelling on the rail infrastructure The settlement of conflicts potentially brings about train delays, which affect the capacity examination of the infrastructure segment examined (within the range from separate station throats to smaller region areas). The simulation can provide data for strategic or tactical rail traffic planning. Examples of mesoscopic simulation tools include *MesoRail*, *SepSimZ* and *SepSimTK*. The *MesoRail* tool [34] is used for traffic simulations within railway stations, whereas *SepSimTK* and *SepSimZ* are specialized in separate traffic simulations on *line tracks* and *station throats*, respectively. The concept of the two latter tools has been described in [5] within the specification of the simulation-based methodologies for the determination of the *line track/station throat* infrastructure capacities.

Since the primary aim of this article is to present innovative algorithms for the automated setup of mesoscopic station throat infrastructure models applicable in separate mesoscopic simulations, attention will be paid only to this simulator type.

II. SIMULATION-BASED METHODOLOGY FOR ASSESSING STATION THROAT CAPACITY

As mentioned above, the station throat capacity can be determined by using the *SepSim-Z* methodology, based on the application of mesoscopic rail traffic simulation. This methodology, which is described in detail in the *SM124 – Railway Capacity Assessment* directive [5], is routinely used by the Czech national authority, the *Railway Infrastructure Administration* (*SŽ, s.o. – Správa železnic*). The directive specifies a number of simulation and analytical methods for the capacity assessment of the various railway infrastructure segments, such as the *line tracks*, *station throats* and *groups of station tracks*.

SepSim-Z original methodology developed by the Czech *Railway Infrastructure Administration*, is based on the concept of analytical rail line capacity calculation proposed by professor Schwanhäußer [20] using the *total waiting times of trains in traffic* as the main traffic indicator W. This concept has been (i) modified for application to the station throat and (ii) transformed into a simulation method – this practically means that selected variables from the analytical formula were transformed into the appropriate parameters of the simulator used. In *SepSim-Z*, the W-indicator value is obtained by processing output data from simulation experiments.

The term *capacity* (of a segment of the rail infrastructure) can be defined as a general ability to provide a certain traffic performance of a certain quality [5]. The capacity can be evaluated within different methodologies by using different indicators (calculated for a specific period and of a specific segment of the infrastructure). Examples include:

- *Waiting times of trains in traffic*, arising from the ride of other trains or shunting rides and not accounted for in the timetable.
- *Infrastructure throughput*, which specifies the feasible number of train runs while maintaining the specified traffic quality level.
- *Occupancy time rate*, mirroring the rate of the use of specific infrastructure segments.
- *Probability of waiting in traffic*, which is the probability that trains in traffic must wait.
- *Train delay increment*, which is the difference between the input delay and output delay with respect to the infrastructure segment examined.

The methodological approach applied by the *SepSim-Z* methodology to assess the station throat capacity can be formulated with some simplification as follows:

(1) The borders of the examined station throat on the track infrastructure and the throat connection to the surrounding are determined.
(2) A mesoscopic model of the station throat infrastructure is set up by using aggregated elements representing groups of switches.

(3) Train runs (or shunting rides) included in the time period analyzed are determined (by using the relevant timetable for instance).
Note: For simplification the term ''train run'' will henceforth also include shunting rides.
(4) The technological times (station headway times) valid for the station throat examined are specified. The above times determine the minimum intervals between two consecutively running trains.
(5) Mesoscopic (stochastic) traffic simulations are performed (e.g., by using *SepSimZ* tool) on the station throat analyzed; this typically includes hundreds of simulation experiment replications belonging to a relevant simulation experiment.
(6) The simulation output data are processed with a focus on the traffic indicator $\bar{w}$, which represents the *mean waiting time of trains in traffic.*
(7) The capacity of the station throat examined is determined based on a comparison between the traffic characteristics obtained from the simulation and related, in particular, to the indicator $\bar{w}$, and the defined limit values.

The steps of the introduced procedure can be described in more detail to illustrate the overall concept of the *SepSim-Z* methodology.

Ad(1) The rail infrastructure model includes the borders of the station throat examined and the elements/tracks to which the station throat is connected are identified.
Ad(2) The mesoscopic infrastructure model construction, which is the focus of this article, is commenced by initialization conversion of the initial (microscopic) station throat model to a primary (mesoscopic) model. This primary model is represented by a directed graph (digraph) whose vertices mirror the switches and track crossings. The interconnections between the switches and track crossings in the infrastructure are represented by directed edges. The primary model is transformed into the target (mesoscopic) model by using partial iterations. A digraph vertex can represent a group of switches. The target infrastructure model will be used to perform the mesoscopic rail traffic simulations.
Ad(3) The train runs (and shunting rides where appropriate) are usually specified via the appropriate timetable. Alternatively, train runs can be specified without a timetable when examining the traffic properties of the station throat for the limiting traffic flow intensities (this approach is suitable for strategic planning of the transport infrastructure for a rather distant time horizon for which no timetables are available).
Ad(4) Depending on the position of the station throat in the wide infrastructure the technological times applied to the infrastructure must be respected when simulating the railway traffic. The technological time mirrors the requirement that the defined station headway times be observed. In fact, the headway times constitute an important traffic parameter in the simulation.
Ad(5) The simulation tool used for the mesoscopic (stochastic) simulation of the traffic on the station throat during a specific period of time (e.g., the peak traffic hours) must, in particular, take into account the following data:
- The time positions of the train runs (specified either in the timetable or in the input train flow generator).
- The train priorities (note that the priorities of the various train categories have been expertly defined [5]).
- Probability distribution of the train delay occurrence at the simulated system input (following the Bernoulli probability distribution pattern [5]).
- Probability distribution of the train delay times at the simulated system input (following the exponential probability distribution pattern [5]).
- The station headway times, mirroring the technological rules applied to the station throat analyzed.

During a simulation experiment, the decision is taken for each train entering the system (reflecting the rail traffic on the station throat under study) whether it will be delayed or not. If it is decided that a particular train will be delayed, a random delay value is assigned to it. The existence of delays can give rise to conflicts between the train runs, and such conflicts are settled, while respecting the train priorities, through shifts in the train time position. The time shifts so generated represent the *waiting times of trains in traffic*, characterized by the traffic indicator w. Each simulation experiment encompasses hundreds or more replications, each providing traffic data for post-simulation statistical processing. The station throat capacity is assessed in the Czech Republic largely by using the *SepSimZ* simulation tool (developed at SŽ, s.o.) working in *MS Excel*.
Ad(6) Comprehensive processing of the output data from simulation experiments, serving to evaluate selected rail traffic characteristics (in particular, the traffic indicator w – *waiting times of trains in traffic*). The following output parameters are followed in this context: (i) the waiting time of each train in traffic, (ii) the sum of the waiting times of all trains in traffic and (iii) the mean waiting time of trains in traffic.
Ad(7) The station throat capacity is assessed mainly by comparison between the mean waiting time of trains in traffic $\bar{w}$ (taking into account the simulated runs of all trains in all replications) and the limit mean waiting times (Table 2). The limit waiting time values for the various train categories are listed in Table 1. This table contains both the *optimum waiting times of trains in traffic* ${}^{C}w_{opt}$ (C∈{Express, Regio, Cargo, Shunt}), which are defined for each train category [5], and the corresponding c*ritical waiting times of trains*

TABLE 1. Specification of limit values related to the waiting times of trains in traffic.

Train category	Optimal waiting times – $^{C}w_{opt}$ [min]	Critical waiting times – $^{C}w_{crit}$ [min]
Express train	0.25 ($^{Express}w_{opt}$)	0.43 ($^{Express}w_{crit}$)
Regional train	0.60 ($^{Regio}w_{opt}$)	1.02 ($^{Regio}w_{crit}$)
Cargo train	1.80 ($^{Cargo}w_{opt}$)	3.06 ($^{Cargo}w_{crit}$)
Shunting set	1.80 ($^{Shunt}w_{opt}$)	3.06 ($^{Shunt}w_{crit}$)

TABLE 2. Classification of station throat capacity reflecting the mean waiting times of trains in traffic.

Station Throat Capacity	Value of the indicator $\bar{w}$
Sufficient	$\bar{w} \leq \bar{w}_{opt}$
Risky	$\bar{w}_{opt} < \bar{w} \leq \bar{w}_{crit}$
Deficient	$\bar{w} > \bar{w}_{crit}$

in traffic $^{C}w_{crit}$, calculated as:

$$^{C}w_{crit} = 1.7 \cdot {}^{C}w_{opt} \quad (1)$$

The optimum mean waiting time of trains in traffic $\bar{w}_{opt}$, obtained from all (N) train runs during the period analysed can be calculated by the formula:

$$\bar{w}_{opt} = Sum_{opt}/N \quad (2)$$

where Sum_{opt} is the sum of the $^{C}w_{opt}$ values for the runs of all trains of all categories, C∈{Express, Regio, Cargo, Shunt}:

$$Sum_{opt} = \Sigma_C(f_C \cdot {}^{C}w_{opt}) \quad (3)$$

where f_C is the frequency of runs of trains in category C.

The critical mean waiting time of trains in traffic $\bar{w}_{crit}$ can be calculated similarly.

In line with the classification in Table 2, the capacity of station throat examined can be graded as *adequate/sufficient*, *inadequate/deficient* or *risky*.

The *SepSim-Z* methodology (described in the directive *SM124* [5]) offers more options for monitoring the (simulated) traffic than as presented above in the basic simplified description. A more detailed description, however, lies beyond the scope of this article. The application of the *SepSim-Z* methodology is illustrated later in a case study showing how the capacity of selected station throat in a minor Czech railway station is assessed.

It is noteworthy that the directive *SM124* also describes a similar methodology, *SepSim-TK* (*Separate Simulation of rail traffic on the line tracks*), which uses mesoscopic simulation for assessing the capacity of line tracks.

III. TRACK INFRASTRUCTURE MODEL

In the methodologies for assessing the capacity of a station throat, the relevant model of the track infrastructure always plays an important role, reflecting the topological and metric conditions of the throat under investigation. The following requirements have been formulated for this type of model and its use within the *SepSim-Z* methodology.

A. OBJECTIVES OF INFRASTRUCTURE MODELING

When modelling station throat infrastructure at a mesoscopic level of detail, it is necessary to ensure that the target model:

- applies the maximum possible level of abstraction to enable realistic modelling of train rides and setting train routes,
- distinguishes between segments of the modelled throat where temporary stays of rail vehicles can take place and segments where such stays are not allowed,
- enables the computation of algorithms detecting all admissible combinations of simultaneously set train routes.

In order to create the desired target infrastructure model, the following original procedure was proposed, which is based on the method of successive transformations of the following mathematical models (graphs):

(a) At first, the *initial microscopic infrastructure model* is constructed as an undirected graph G_0 based on a schematic track layout.

(b) Next, the *primary (atomic) mesoscopic infrastructure model* is formed as the (primary) directed acyclic graph G_P – a digraph with vertices called *atomic vertices*, each representing a switch, a track crossing or a sojourn track element. The digraph G_P is obtained by conversion of graph G_0.

(c) Finally, the *target hybrid mesoscopic infrastructure model* is set up by a multi-stage process as a directed graph G_H containing what is called *meso-vertices* (or, alternatively, aggregated vertices) and potentially also atomic vertices. Unlike atomic vertices, the meso-vertices represent groups of switches and/or track crossings.

B. INITIAL MICROSCOPIC INFRASTRUCTURE MODEL

Motivation for setting up the initial microscopic infrastructure layout model within step (a) is obtaining a rigorous formal specification of the track infrastructure topology. For this, the official track layout must be available (which is commonplace in railway companies). A layout consists of 2 parts: the graphical part and the data part. The former is a schematic representation of the track topology. The data part contains information on the lengths of the infrastructure elements (tracks, switches, track crossings) as well as the mileage positions of selected equipment (railway signal devices, hectometer posts, switches, track crossings, etc.). An illustrative example of a fragment of the railway station track layout is shown in Fig. 1. The information from the track layout can be used to expertly set up the initial (microscopic) infrastructure model as an undirected graph G_0, representing the rail yard elements at the microscopic level of detail (an example of such a model is presented in Fig. 2).

TABLE 3. Specification of the undirected graph G_0 – the initial (schematic) model of the rail infrastructure.

Symbols	Specifications
G_0	The undirected graph $G_0 = (V,E,\varphi,\omega)$
$V(G_0)$	The set of *vertices* of graph G_0
$E(G_0)$	The set of *edges* of the graph G_0 $E(G_0) = E_{branch}(G_0) \cup E_{sojourn}(G_0) \cup E_{conn}(G_0)$ $E_{branch}(G_0) \cap E_{sojourn}(G_0) \cap E_{conn}(G_0) = \emptyset$, pairwise disjoint subsets of $E(G_0)$ The set $E_{branch}(G_0)$ contains *branch edges* (reflecting parts of crossings or switches) The set $E_{sojourn}$ contains *sojourn edges* (mirroring tracks that can serve as sojourn elements for rail vehicles) The set $E_{conn}(G_0)$ contains *connecting edges* (reflecting connecting track elements)
φ	The *incidence function* related to the graph G_0 φ: $E(G_0) \rightarrow \{(v_i,v_j) \mid (v_i,v_j) \in V(G_0) \times V(G_0), v_i \neq v_j\}$ The symbol (v_i,v_j) denotes an unordered pair of vertices (undirected edge) $\forall\, v_i \in V(G_0)$: $\deg(v_i) \in \{1,2,3\}$, $m \leq \lfloor (3/2)\, n \rfloor$ for $n \geq 4$, $n = \lvert V(G_0) \rvert$, $m = \lvert E(G_0) \rvert$
ω	The *edge weight function* related to graph G_0 ω: $E(G_0) \rightarrow R^+$ (the set of positive real numbers)

The specification of this graph type is given in Table 3 and a detailed illustrative description of a particular instance is presented later in the case study. Transformations specified in Fig. 3 are used during the construction of the switch and track crossing models within graph G_0. The following symbols are used to represent the various switch and track crossing types: Y – (*simple*) *switch*, X – *track crossing*, D – *double slip switch*, S – *single slip switch*. The tracks shown in the layout are represented by undirected edges in the graph G_0.

Edges represent tracks or track elements in graph G_0. Three edge types are discriminated in the set $E(G_0)$, representing: (i) track elements of switches and track crossings ($E_{branch}(G_0) \subset E(G_0)$); (ii) tracks or track elements on which rail vehicle sojourn is feasible ($E_{sojourn}(G_0) \subset E(G_0)$); and (iii) connecting track elements ($E_{conn}(G_0) \subset E(G_0)$). If appropriate, G_0 can be constructed as an edge-weighted graph where the edge lengths represent the matching track element lengths.

Note.: For simplification of the explanation, the general term 'track element' will henceforth mean a complete track or a segment thereof or the track part of a switch or a track crossing.

C. PRIMARY MESOSCOPIC INFRASTRUCTURE MODEL

Step (b) serves to transform the microscopic infrastructure model to a primary/atomic mesoscopic model, primarily focusing on the specification (at the mesoscopic level of detail) of the interconnected switches, track crossings and sojourn track elements (particularly within a station throat and its immediate surrounding).

TABLE 4. Specification of digraph G_P – the model of rail infrastructure containing atomic vertices.

Symbols	Specifications
G_P	The digraph $G_P = (V,E,\varphi,\kappa)$ The primary acyclic digraph G_P represents a result related to the transformation of the relevant undirected graph G_0 (representing an initial model of rail infrastructure. The digraph G_P encapsulates (atomic) vertices reflecting what is called *atomic track elements*.
$V(G_P)$	The set of vertices of the digraph G_P $V(G_P) = {}^{Y}V(G_P) \cup {}^{X}V(G_P) \cup {}^{S}V(G_P) \cup {}^{D}V(G_P) \cup {}^{T}V(G_P)$ ${}^{Y}V(G_P) \cap {}^{X}V(G_P) \cap {}^{S}V(G_P) \cap {}^{D}V(G_P) \cap {}^{T}V(G_P) = \emptyset$, pairwise disjoint subsets of $V(G_P)$ The subsets contain *atomic vertices* reflecting specific subgraphs of the initial undirected graph G_0, i.e., *single* rail *switches* (${}^{Y}V(G_P)$), rail *crossings* (${}^{X}V(G_P)$), *single slip switches* (${}^{S}V(G_P)$) and *double slip switches* (${}^{D}V(G_P)$). In addition, *sojourn* track elements are mirrored by the elements of ${}^{T}V(G_P) = {}^{BT}V(G_P) \cup {}^{IT}V(G_P)$ where ${}^{BT}V(G_P) \cap {}^{IT}V(G_P) = \emptyset$; ${}^{BT}V(G_P)$ contains border (outer) sojourn elements and ${}^{IT}V(G_P)$ includes interior (inner) sojourn elements.
$E(G_P)$	The set of directed edges of the digraph G_P
φ	The *incidence function* related to the digraph G_P φ: $E(G_P) \rightarrow \{[v_i,v_j] \mid [v_i,v_j] \in V(G_P) \times V(G_P), v_i \neq v_j\}$ The symbol $[v_i,v_j]$ denotes an ordered pair of vertices (directed edge) $\forall\, v_i \in (V(G_P) - {}^{T}V(G_P))$: $\text{indeg}(v_i) \in \{1,2\}$, $\text{outdeg}(v_i) \in \{1,2\}$ $\forall\, v_i \in {}^{T}V(G_P)$: $\text{indeg}(v_i) \in \{0,1\}$, $\text{outdeg}(v_i) \in \{0,1\}$ $(\text{indeg}(v_i) + \text{outdeg}(v_i)) \in \{1,2\}$
κ	The *vertex weight function* related to the digraph G_P κ: $V(G_P) \rightarrow R^+$ (the set of positive real numbers)

This primary model is represented by a directed acyclic graph G_P, the specification of which is listed in Table 4. This digraph contains a set of vertices reflecting:

- the switches and track crossings contained in graph G_0 (where they are represented by simple subgraphs); different graphical vertex symbols are used in digraph G_P diagram (Figs. 3, 4),
- selected edges in the graph G_0 representing the various tracks or track elements on which the sojourn of rail cars is possible; such vertex types are graphically represented by rectangles in digraph G_P diagram (Figs. 3, 4).

The directed edges in digraph G_P represent only logical connections between the vertices and do not mirror any other track elements.

The above primary model is the basis for its subsequent transformations aimed to apply a higher degree of abstraction when modelling station throats.

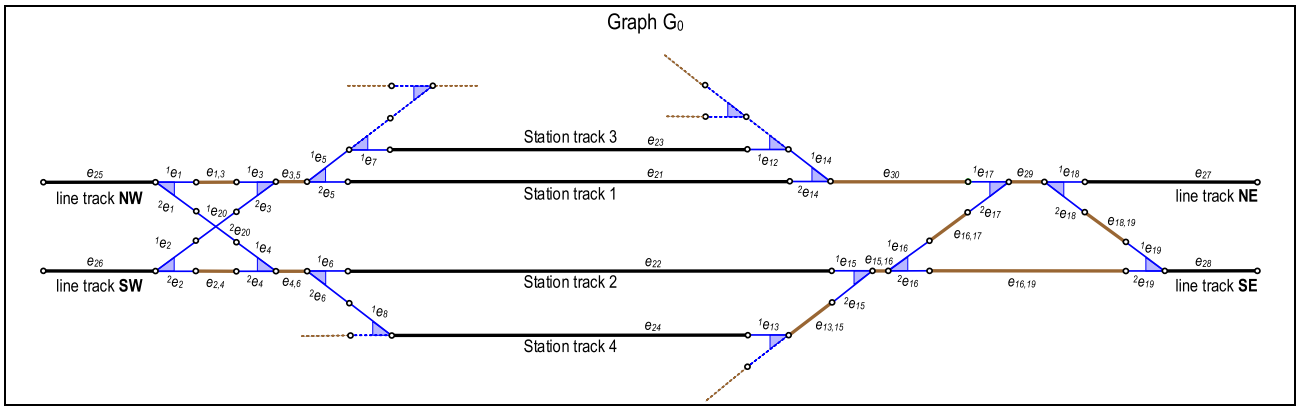

FIGURE 2. Initial microscopic model (graph G_0) of an illustrative rail yard track infrastructure.

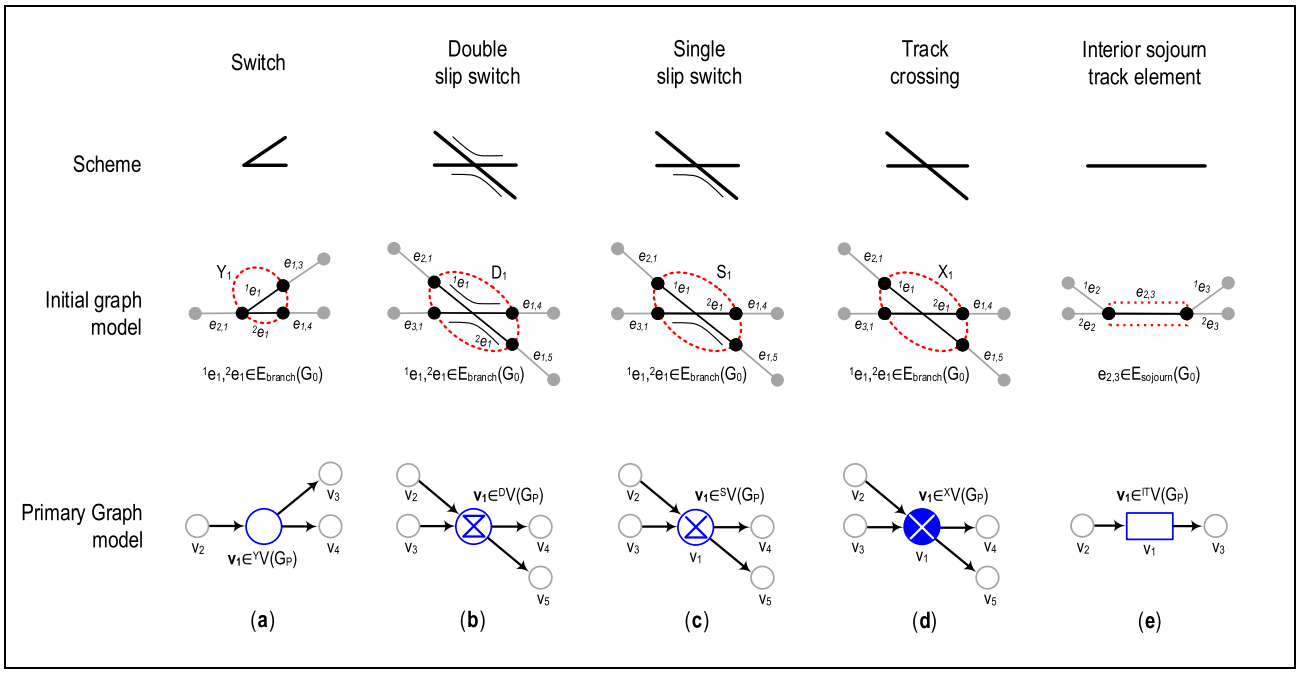

FIGURE 3. Conversions of sub-models (reflecting switches and tracks crossings) into different graph models.

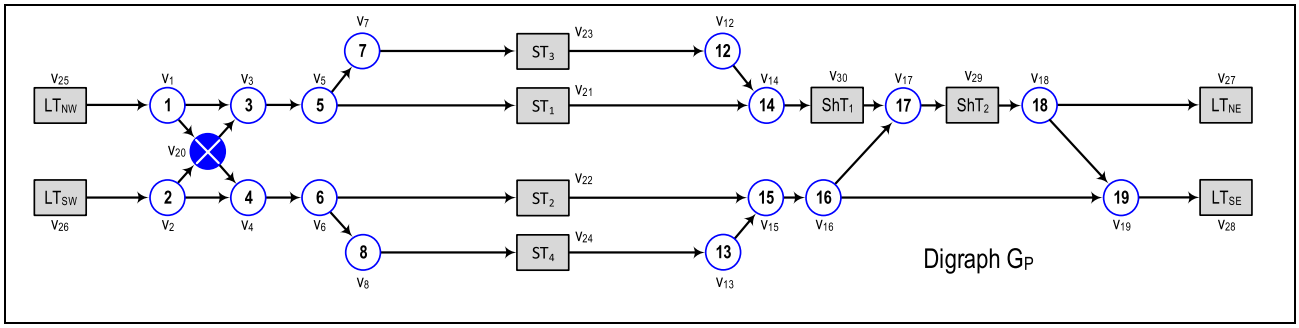

FIGURE 4. Primary mesoscopic model (digraph G_P) of an illustrative rail yard layout including two station throats.

The vertex set $V(G_P)$ differentiates between 5 vertex types representing: (i) simple rail switches (${}^{Y}V(G_P) \subset V(G_P)$), (ii) track crossings (${}^{X}V(G_P) \subset V(G_P)$), (iii) single slip switches (${}^{S}V(G_P) \subset V(G_P)$), (iv) double slip switches (${}^{D}V(G_P) \subset V(G_P)$) and (v) tracks/track elements on which sojourn of rail vehicles is feasible (${}^{T}V(G_P) \subset V(G_P)$). The set ${}^{T}V(G_P)$ meets the relation ${}^{T}V(G_P) = {}^{BT}V(G_P) \cup {}^{IT}V(G_P)$ where ${}^{BT}V(G_P) \cap {}^{IT}V(G_P) = \emptyset$. The set ${}^{BT}V(G_P)$ includes

vertices representing border (outer) sojourn track elements adjacent to the station throat modelled and the set ${}^{\mathrm{IT}}\mathrm{V}(\mathrm{G_P})$ includes vertices representing interior (inner) sojourn track elements of the station throat modelled.

Where appropriate, $\mathrm{G_P}$ can be set up as a vertex-weighted digraph in which the vertex weights represent the lengths of the appropriate track elements that must be traversed when passing the relevant switch or track crossing.

The edge directions are selected by applying a strategy that takes into account the topological situation in the track layout. In a specific station throat model, all edges are typically directed either away from the line tracks (modelled through vertices in the set $\Lambda \subset {}^{\mathrm{BT}}\mathrm{V}(\mathrm{G_P})$) towards the station tracks (modelled through vertices in the set $\Omega \subset {}^{\mathrm{BT}}\mathrm{V}(\mathrm{G_P})$) or the other way round, where ${}^{\mathrm{BT}}\mathrm{V}(\mathrm{G_P}) = \Lambda \cup \Omega$, $\Lambda \cap \Omega = \emptyset$. Examples of vertex membership in the sets Λ, Ω are given in section V.

D. TARGET HYBRID MESOSCOPIC INFRASTRUCTURE MODEL

The purpose of the iterative creation of the target hybrid station throat infrastructure model based on the primary mesoscopic model (primary digraph $\mathrm{G_P}$) is a stepwise grouping of adjacent vertices into *meso-vertices* (aggregated vertices) in a hybrid digraph $\mathrm{G_H}$. The specification of this directed graph is shown in Table 5. The aim of the iterative aggregations (based on rules that are described later) is to attain the simplest feasible and credible target model of the infrastructure. This model must enable us to realistically simulate the conditions of setting train routes (or shunting routes) through station throat, where the interlocking system locks not only the track elements (switches, track crossings) that are used by the track vehicles but also selected adjacent track elements. The initial topology of the hybrid infrastructure model is identical to the topology of the appropriate digraph $\mathrm{G_P}$. The transformation iterations of digraph $\mathrm{G_H}$ within the step (c) can be terminated if the aggregation of the vertices cannot be continued any more (based on the rules). The resulting digraph $\mathrm{G_H}$ topology is then used in the simulation model intended for examining rail traffic on the relevant station throat.

If required, $\mathrm{G_H}$ can be set up as a vertex-weighted digraph where the weights of the vertices represent the lengths of the track elements that must be traversed when passing the relevant switch or track crossing. The weights of the vertices in the set ${}^{\mathrm{IT}}\mathrm{V}(\mathrm{G_H})$ also play a role when assessing the admissibility of the sojourn of trains or shunted wagons (with their lengths) on the interior sojourn track elements of the station throat, particularly in the context of shunting.

The specification of digraph $\mathrm{G_H}$ is nearly identical to that of digraph $\mathrm{G_P}$, with a single exception, which is extension of the vertex set $\mathrm{V}(\mathrm{G_H})$ with the set ${}^{\mathrm{M}}\mathrm{V}(\mathrm{G_H})$ consisting of meso-vertices:

$$V(G_{\mathrm{H}}) = {}^{\mathrm{Y}}V(G_{\mathrm{H}}) \cup^{\mathrm{X}} V(G_{\mathrm{H}}) \cup^{\mathrm{S}} V(G_{\mathrm{H}}) \cup^{\mathrm{D}} V(G_{\mathrm{H}}) \cup^{\mathrm{T}} V(G_{\mathrm{H}}) \cup^{\mathrm{M}} V(G_{\mathrm{H}})$$

TABLE 5. Specification of digraph $\mathrm{G_H}$ – the (hybrid) model containing meso-vertices and atomic vertices.

Symbols	Specifications
$\mathrm{G_H}$	The (hybrid) digraph $\mathrm{G_H} = (\mathrm{V},\mathrm{E},\varphi,\kappa)$ The digraph $\mathrm{G_H}$ represents a result related to the transformation of the relevant digraph $\mathrm{G_P}$ (composed of atomic vertices). The digraph $\mathrm{G_H}$ contains *atomic vertices* (reflecting selected atomic vertices of the digraph $\mathrm{G_P}$) and potentially also *meso-vertices* (reflecting specific subgraphs of the relevant digraph $\mathrm{G_P}$).
$\mathrm{V}(\mathrm{G_H})$	The set of vertices of the digraph $\mathrm{G_H}$ $\mathrm{V}(\mathrm{G_H}) = {}^{\mathrm{Y}}\mathrm{V}(\mathrm{G_H}) \cup^{\mathrm{X}} \mathrm{V}(\mathrm{G_H}) \cup^{\mathrm{S}} \mathrm{V}(\mathrm{G_H}) \cup^{\mathrm{D}} \mathrm{V}(\mathrm{G_H}) \cup^{\mathrm{T}} \mathrm{V}(\mathrm{G_H}) \cup^{\mathrm{M}} \mathrm{V}(\mathrm{G_H})$ ${}^{\mathrm{Y}}\mathrm{V}(\mathrm{G_H}) \cap^{\mathrm{X}} \mathrm{V}(\mathrm{G_H}) \cap^{\mathrm{S}} \mathrm{V}(\mathrm{G_H}) \cap^{\mathrm{D}} \mathrm{V}(\mathrm{G_H}) \cap^{\mathrm{T}} \mathrm{V}(\mathrm{G_H}) \cap^{\mathrm{M}} \mathrm{V}(\mathrm{G_H}) = \emptyset$, pairwise disjoint subsets of $\mathrm{V}(\mathrm{G_H})$ The subsets contain vertices reflecting atomic track elements, i.e., *single* rail *switches* (${}^{\mathrm{Y}}\mathrm{V}(\mathrm{G_H})$), rail *crossings* (${}^{\mathrm{X}}\mathrm{V}(\mathrm{G_H})$), *single slip switches* (${}^{\mathrm{S}}\mathrm{V}(\mathrm{G_H})$), *double slip switches* (${}^{\mathrm{D}}\mathrm{V}(\mathrm{G_H})$) and *sojourn* track elements (${}^{\mathrm{T}}\mathrm{V}(\mathrm{G_H})$). ${}^{\mathrm{T}}\mathrm{V}(\mathrm{G_H}) = {}^{\mathrm{BT}}\mathrm{V}(\mathrm{G_H}) \cup {}^{\mathrm{IT}}\mathrm{V}(\mathrm{G_H})$, where ${}^{\mathrm{BT}}\mathrm{V}(\mathrm{G_H}) \cap {}^{\mathrm{IT}}\mathrm{V}(\mathrm{G_H}) = \emptyset$; ${}^{\mathrm{BT}}\mathrm{V}(\mathrm{G_H})$ contains border (outer) sojourn elements and ${}^{\mathrm{IT}}\mathrm{V}(\mathrm{G_H})$ includes interior (inner) sojourn elements. The set ${}^{\mathrm{M}}\mathrm{V}(\mathrm{G_H})$ is composed of so-called *meso-vertices* (or aggregated vertices) reflecting specific subgraphs of the digraph $\mathrm{G_P}$ A special case of the digraph $\mathrm{G_H}$ topology represents its instance with a specific feature: ${}^{\mathrm{M}}\mathrm{V}(\mathrm{G_H}) = \emptyset$, i.e., the topology is equal to a topology of a corresponding primary digraph $\mathrm{G_P}$
$\mathrm{E}(\mathrm{G_H})$	The set of directed edges of the digraph $\mathrm{G_H}$ The directed edges of $\mathrm{G_H}$ reflect selected directed edges from $\mathrm{E}(\mathrm{G_P})$
φ	The *incidence function* related to the digraph $\mathrm{G_H}$ φ: $\mathrm{E}(\mathrm{G_H}) \rightarrow \{[\mathrm{v_i},\mathrm{v_j}] \mid [\mathrm{v_i},\mathrm{v_j}] \in \mathrm{V}(\mathrm{G_H}) \times \mathrm{V}(\mathrm{G_H}),\ \mathrm{v_i} \neq \mathrm{v_j}\}$ The symbol $[\mathrm{v_i},\mathrm{v_j}]$ denotes an ordered pair of vertices (directed edge)
κ	The *vertex weight function* related to the digraph $\mathrm{G_H}$ κ: $\mathrm{V}(\mathrm{G_H}) \rightarrow \mathrm{R}^+$ (the set of positive real numbers)
$\mathrm{Succ}(\mathrm{v_i})$	The set of adjacent vertices-successors of the vertex $\mathrm{v_i} \in \mathrm{V}(\mathrm{G_H})$ $\mathrm{Succ}(\mathrm{v_i}) = \{\mathrm{v_j} \mid [\mathrm{v_i},\mathrm{v_j}] = \varphi(\mathrm{e_u}),\ \mathrm{e_u} \in \mathrm{E}(\mathrm{G_H})\}$, $\mathrm{Succ}(\mathrm{v_i}) \subset \mathrm{V}(\mathrm{G_H})$, $\lvert\mathrm{Succ}(\mathrm{v_i})\rvert = \mathrm{outdeg}(\mathrm{v_i})$
$\mathrm{Pred}(\mathrm{v_i})$	The set of adjacent vertices-predecessors of the vertex $\mathrm{v_i} \in \mathrm{V}(\mathrm{G_H})$ $\mathrm{Pred}(\mathrm{v_i}) = \{\mathrm{v_j} \mid [\mathrm{v_j},\mathrm{v_i}] = \varphi(\mathrm{e_u}),\ \mathrm{E}(\mathrm{G_H})\}$, $\mathrm{Pred}(\mathrm{v_i}) \subset \mathrm{V}(\mathrm{G_H})$, $\lvert\mathrm{Pred}(\mathrm{v_i})\rvert = \mathrm{indeg}(\mathrm{v_i})$

Note: The final topology of the target digraph $\mathrm{G_H}$ forms a basis for the implementation of the relevant infrastructure submodel, which forms part of the appropriate mesoscopic simulator (such as *SepSimZ* tool).

IV. ALGORITHMS FOR AUTOMATED FORMATION OF THE TARGET INFRASTRUCTURE MODEL

The main issue of this article is the design, development, and verification of innovative graph algorithms that specialize in automatic forming a target model of the station throat infrastructure.

A. ALGORITHM DEVELOPMENT OBJECTIVES

The main goal of the development of the innovated algorithms, which are aimed at performing consecutive transformations of the topology of the mesoscopic hybrid infrastructure model (digraph G_H), was to achieve maximum admissible topological simplification. This simplification contributes to a faster and more efficient construction of the mesoscopic simulation model focused on rail traffic simulation within the station throat area examined. Certainly, the final (simplified) topology of digraph G_H must allow realistic modelling of train rides and setting train routes.

B. TRANSFORMATION RULES

The conditions and the related topology change types (applied to digraph G_H) are specified below in *Rules* $A - D$. The rule definitions use the formalism described in Table 5.

Initially published in [35] and [36], the concept of the rules described below eventually required modifications and innovations. The feasibility of each rule had also to be formally mathematically specified – the initial textual specifications were not unambiguous and enabled multiple interpretations. In practice, the rules were applied manually only (frequently without checking the correctness of the target model topology). So, algorithms in support of the automated application of *Rules* $A - D$ were devised, implemented and tested in efforts to enhance the *SepSim-Z* methodology.

Rule A

If a vertex $v_i \in V(G_H)$ has a single successor $v_j \in V(G_H)$, then the vertices v_i and v_j can be aggregated into a new meso-vertex (for a graphic illustration see Fig. 5a). This aggregation can be made if $v_i \notin ({}^{T}V(G_H) \cup {}^{X}V(G_H))$, $v_j \in Succ(v_i)$, $|Succ(v_i)| = 1$, and $v_j \notin ({}^{T}V(G_H) \cup {}^{X}V(G_H))$.

Rule B

If a vertex $v_i \in V(G_H)$ has a single predecessor $v_j \in V(G_H)$, then the vertices v_i and v_j can be aggregated into a new meso-vertex (for a graphic illustration see Fig. 5b). This aggregation can be made if $v_i \notin ({}^{T}V(G_H) \cup {}^{X}V(G_H))$, $v_j \in Pred(v_i)$, $|Pred(v_i)| = 1$, and $v_j \notin ({}^{T}V(G_H) \cup {}^{X}V(G_H))$.

Rule C

If the vertex $v_i \in V(G_H)$ has 2 (and only 2) successors $v_j, v_k \in V(G_H)$ and $v_j \in V(G_H)$ has 2 (and only 2) predecessors $v_i, v_k \in V(G_H)$, then the vertices v_i and v_j can be aggregated into a new meso-vertex (for a graphic illustration see Fig. 5c). This aggregation can be made if $v_i \notin ({}^{T}V(G_H) \cup {}^{X}V(G_H))$, $v_j \in Succ(v_i)$, $v_j \notin ({}^{T}V(G_H) \cup {}^{X}V(G_H))$, $|Succ(v_i)| = |Pred(v_j)| = 2$, $|Succ(v_i) \cap Pred(v_j)| = 1$, $v_k \notin {}^{T}V(G_H)$, $v_i \notin Succ(v_k)$ and $v_k \notin Succ(v_j)$.

Rule D

If a vertex $v_i \in {}^{X}V(G_H)$ has one successor $v_j \in V(G_H)$ that is also its predecessor, then the vertices v_i and v_j can be aggregated into a new meso-vertex (for a graphic illustration see Fig. 5d). This aggregation can be made if $v_j \in Succ(v_i)$, $v_j \in Pred(v_i)$ and $v_j \notin ({}^{T}V(G_H) \cup {}^{X}V(G_H))$.

The use of the rules is demonstrated in an example presented in Figs. 6, 7. The whole model of the demonstration station (involving 2 station throats – Fig. 4) is used to present an adequate number of vertex aggregations.

The application of any of the rules is marked with the appropriate identifier whose index matches the order of the executed aggregation. For simplification, the changes in digraph G_H topology are shown after multiple transformation iterations. The last image in Fig. 7 represents an interpretation of selected vertices in digraph G_H (after the 10th transformation iteration) on graph G_0.

C. FEATURES OF MESO-VERTICES

The target infrastructure model topology (digraph G_H), obtained by a series of primary digraph G_P transformations (following the *Rules* $A - D$), must enable simultaneous track routes setting in the simulator such as faithfully reflects the possibilities of simultaneous routing on real/modelled station throat. Only those switches (or crossings) are aggregated in any meso-vertex that must be simultaneously locked when setting the track routes. In other words, if one switch or crossing represented by a meso-vertex is occupied by a train run, then no other switches or crossings represented by the same meso-vertex must be occupied by a different train run.

Note: If the consecutive automated aggregations give rise to meso-vertices representing geographically very extensive parts of the station throat, the meso-vertices may be subsequently decomposed based on an expert's decision if required.

D. MESOINFRA SOFTWARE TOOL

The software *MesoINFRA* was developed at the University of Pardubice as a supportive tool primarily determined for preparations of station throat infrastructure models utilized within *SepSim-Z* methodology.

The mentioned tool supports the following types of functions:

- Loading the initial microscopic infrastructure model (an undirected edge-weighted graph G_0 based on a schematic track layout) reflecting the railway station under investigation. That model is typically obtained from the relevant railway company's information system (e.g., in the Czech Republic from IS KANGO that is managed by Railway Infrastructure Administration).
- Converting the initial microscopic model to a primary (atomic) mesoscopic model represented by a vertex-weighted directed acyclic graph G_P.
- Making automatic successive transformations of the primary mesoscopic model to a target hybrid model G_H (typically containing a mixture of atomic vertices and meso-vertices). The result of each individual transformation can be visualized through a corresponding diagram reflecting the current topology of the G_H graph. The implementation of this function includes partial implementations of algorithms implementing the Rules A–D and has been used to advantage in debugging these algorithms.

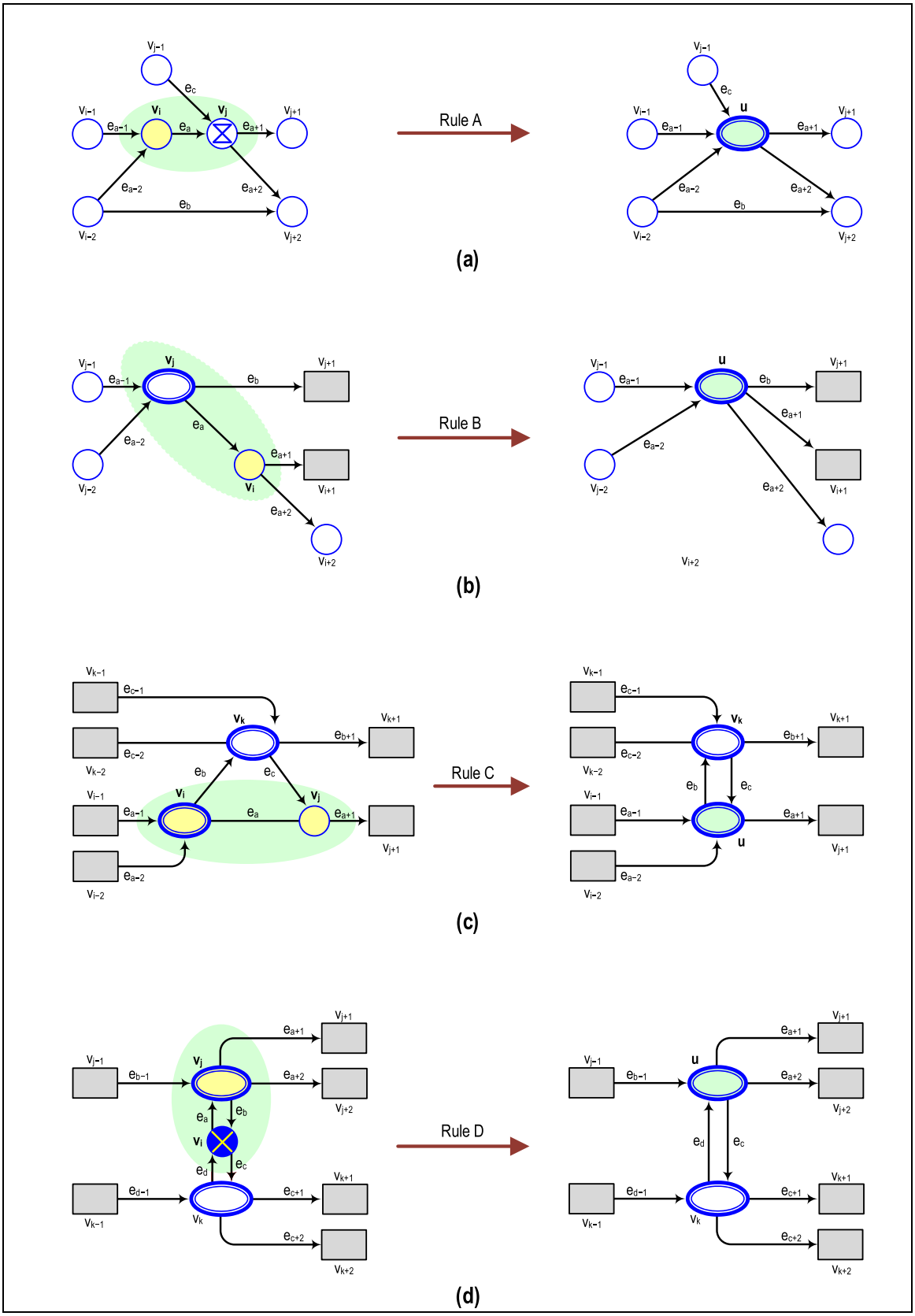

FIGURE 5. Illustrations of aggregation rules within mesoscopic models (digraph G_H) of track infrastructure.

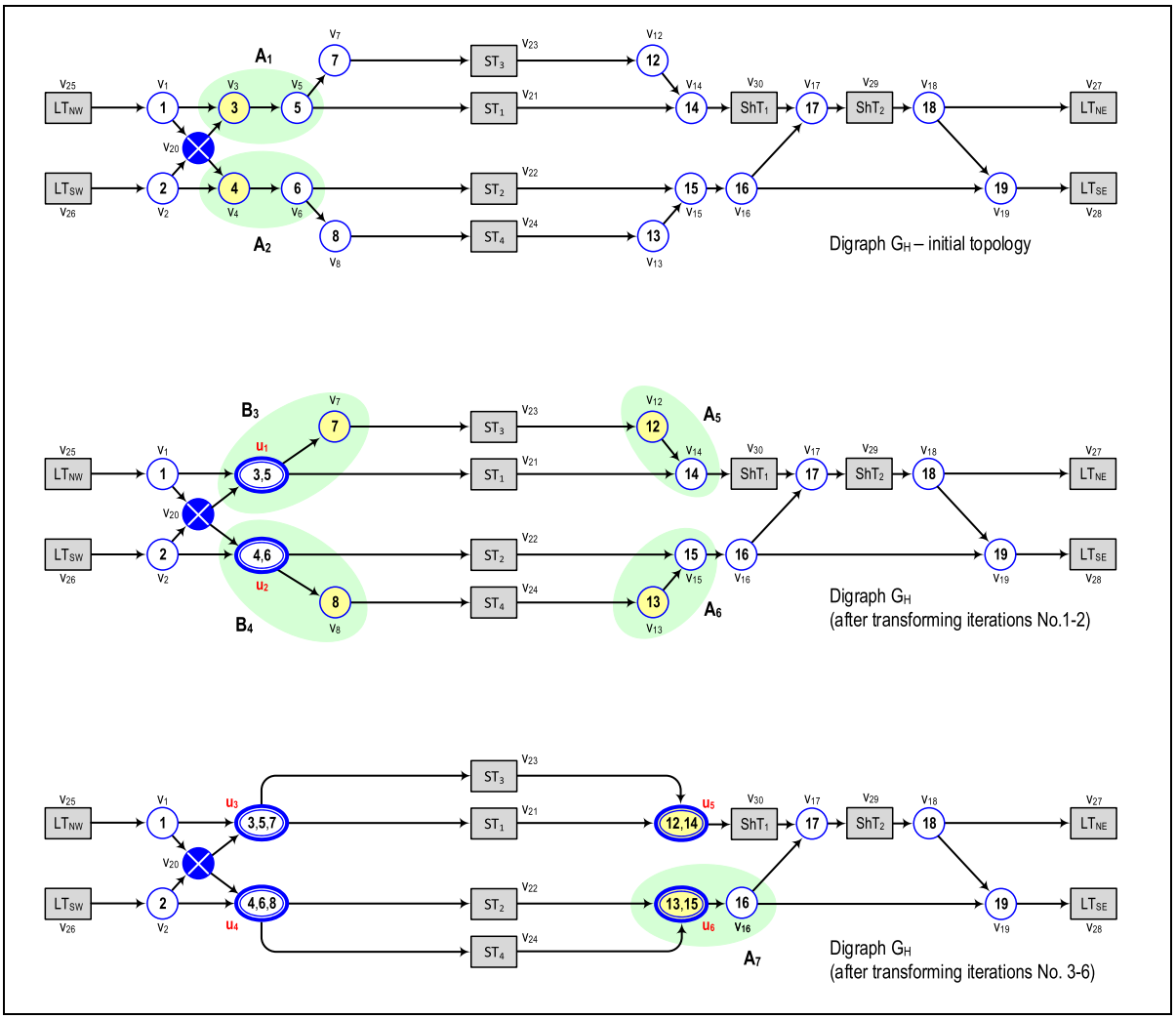

FIGURE 6. Illustrative applications of aggregation rules (iterations 1–6).

- Exporting the target hybrid infrastructure model to *SepSimZ* tool which utilizes the mentioned model in simulations mirroring rail traffic on the station throat under study.
- Computing all admissible single train routes and additionally all permissible combinations of simultaneously set train routes. These auxiliary calculations allow to get an overview of all variants of setting routes on the investigated station throat.

The tool was also actively used to test the developed algorithms (implementing Rules A–D). The corresponding verification and validation process is also described below.

The control panel of *MesoINFRA* software and illustrative models of the station throats are shown in Figs. 8, 9. A more detailed description of this tool and its functionalities is beyond the scope of this article.

E. IMPLEMENTATION OF ALGORITHMS

The implementations of algorithms performing aggregations of vertices within the G_H digraph can be divided into the following three parts, which are focused on:

- Identification of compliance with the conditions for those relevant vertex pairs $v_i, v_j \in V(G_H)$ to which any of the rules for their aggregation can be applied; this is done by using the routines: *Find_A_B*, *Find_C* and *Find_D*, which seek always for one specific vertex pair.
- Aggregation of the vertex pair $v_i, v_j \in V(G_H)$ found in the previous step into a new meso-vertex $u \in {}^{M}V(G_H)$ by using the routine *Aggreg_Two_Vertices*.
- Cyclic executions of the above-mentioned routines as long as the aggregation rules can be applied; this is done by using the routine *Meso_Vertices_Construction*.

The implementation concept is formalized using pseudocode in Algorithm 1. The function *Find_A_B* systematically browses the subset of vertices $V(G_H)$ that does not contain vertices representing sojourn track elements or track crossings. The applicability of *Rule A* is first evaluated for each vertex $v_i \in (V(G_H) - ({}^{T}V(G_H) \cup {}^{X}V(G_H)))$ processed. If *Rule A* is inapplicable, the applicability of *Rule B* is examined. The first vertex v_i the processing of which revealed the applicability of *Rule A* or *Rule B* is identified by the function as a vertex that can be aggregated with the indicated vertex v_j.

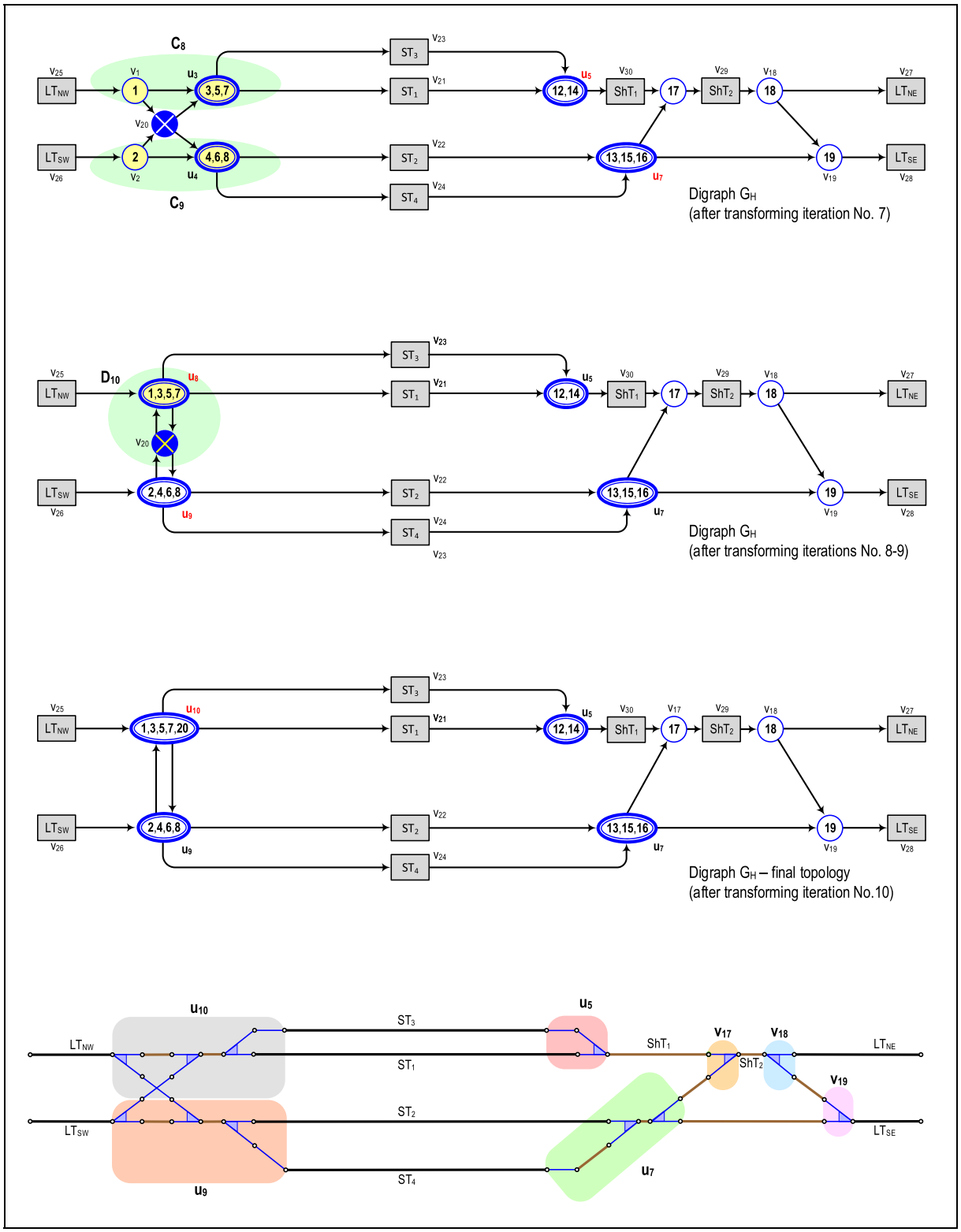

FIGURE 7. Illustrative applications of aggregation rules (iterations 7–10).

The function *Find_C* works similarly to the previous function, only it is *Rule C* the applicability of which is examined.

Unlike the previous functions, the function *Find_D* browses the set of vertices ${}^{X}V(G_H) \subset V(G_H)$ whose elements represent track crossings. The validity of the conditions

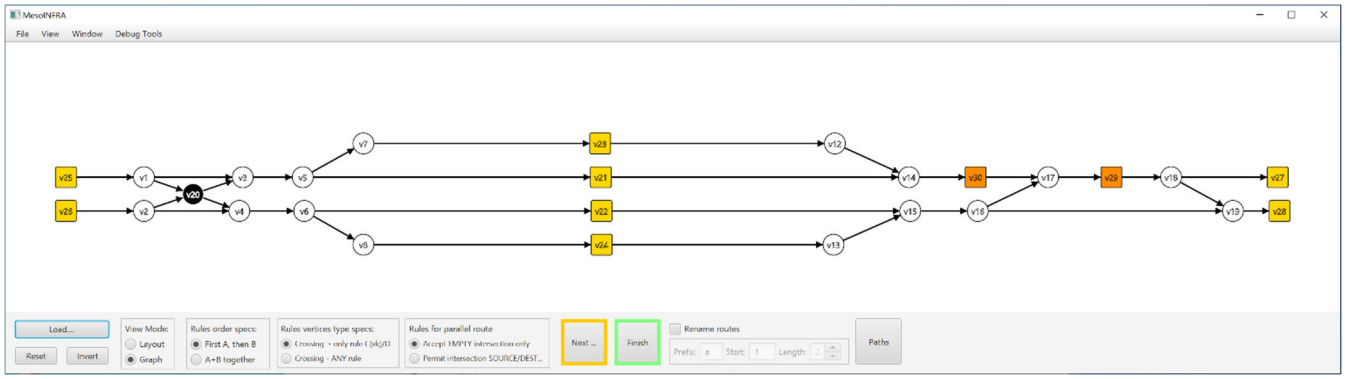

FIGURE 8. Primary/atomic model of the station infrastructure constructed within MesoINFRA tool.

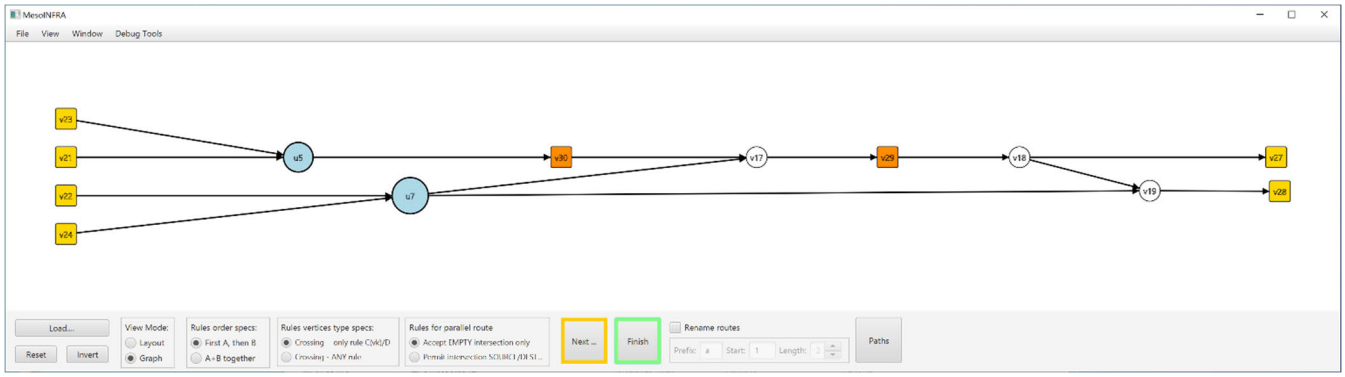

FIGURE 9. Hybrid model of the station throat EAST computed within MesoINFRA tool.

required for *Rule D* to be applicable is tested for each vertex $v_i \in {}^{X}V(G_H)$ being processed. If the condition is met, this fact is indicated for a subsequent aggregation of the vertex v_i with the matching vertex $v_j \in V(G_H)$.

The function *Aggreg_Two_Vertices* individually aggregates two vertices v_i,$v_j \in V(G_H)$. The process encompasses 5 procedures: (i) removal of the vertices v_i and v_j from the set $V(G_H)$; (ii) removal of all edges that are incident with the vertices v_i and v_j from the set $E(G_H)$; (iii) creation of a new meso-vertex u; (iv) insertion of the meso-vertex u into the set ${}^{M}V(G_H)$; and (v) insertion of new edges to the set $E(G_H)$ – the new edges will correctly address the "connection" of the meso-vertex u to its surrounding in a manner similar to that through which the vertices v_i a v_j were connected to their surroundings.

The control function *Meso_Vertices_Construction* performs the following in each of the 3 consecutive cycles: (i) it finds vertex pairs for their aggregation, and (ii) aggregates the pairs identified. The first cycle tests the applicability of *Rules* $A - B$, the next 2 cycles test the applicability of *Rule C* and *Rule D*. Each of the cycles is terminated if no vertex pair meeting the condition for aggregation according to the rule is present in the graph any more. The order of the partial cycles reflects a strategy of the process where the simpler rules for aggregation are applied before the more complex rules. The main cycle of the function is terminated if none of the *Rules* $A - D$ can be applied any more. The final topology of the target digraph G_H is available once the computation of this function has been terminated.

The function parameters are labelled with the following prefix symbols: '↓', denoting an input parameter, '↑', denoting an output parameter, and '↓↑', denoting an input-output parameter. The algorithm used an auxiliary function *Get_Vertex*, described in Table 6.

F. SEARCH FOR ADMISSIBLE ROUTES ON THE MODEL OF INFRASTRUCTURE

When computing in the *MesoINFRA* tool all admissible track routes on which simulated train run is feasible, directed paths on digraph G_H are sought. It holds for the above paths (the maximum number of which is denoted k) that their starting and destination vertices are from the set ${}^{T}V(G_H)$. The topology of all the above paths can be computed by using the *Depth-First Search* algorithm (*DFS*) with backtracking [37]. During the computation, the return vertex addresses are saved in an auxiliary stack data structure, where the LIFO (Last In First Out) strategy is applied when inserting and removing the elements-vertices.

The rules for admissible passage through the currently processed vertex must be applied when computing the *DFS*

Algorithm 1 Construction of Meso-Vertices in the Models of Rail Infrastructure

```
01 function Meso_Vertices_Construction(↓↑G_H)
02   repeat
03     finished←true
04     repeat
05       Find_A_B(↓G_H, ↑v_i, ↑v_j, ↑rslt)
06       if rslt ≠ none then
07         Aggreg_Two_Vertices(↓↑G_H, ↓v_i, ↓v_j)
08         finished←false
09       end
010    until rslt = none
011    repeat
012      Find_C(↓G_H, ↑v_i, ↑v_j, ↑rslt)
013      if rslt ≠ none then
014        Aggreg_Two_Vertices(↓↑G_H, ↓v_i, ↓v_j)
015        finished←false
016      end
017    until rslt = none
018    repeat
019      Find_D(↓G_H, ↑v_i, ↑v_j, ↑rslt)
020      if rslt ≠ none then
021        Aggreg_Two_Vertices(↓↑G_H, ↓v_i, ↓v_j)
022        finished← false
023      end
024    until rslt = none
025  until finished
026 end
027 function Find_A_B(↓G_H, ↑v_i, ↑v_j, ↑rslt)
028   rslt←none
029   foreach v_i ∈ (V(G_H) − (^T V(G_H) ∪^X V(G_H)))
030     cycle←1
031     repeat
032       if cycle = 1 then
033         Z←Succ(v_i)
034       else
035         Z←Pred(v_i)
036       end
037       if |Z| = 1 then
038         Get_Vertex(↓Z, ↑v_j)
039         if v_j ∉ (^T V(G_H) ∪^X V(G_H)) then
040           rslt←found
041           exit
042         end
043       end
044       cycle←cycle+1
045     until cycle>2
046   end
047 end
```

algorithm. The basic rules of admissible passage through the atomic type vertices are listed in Table 7, referring to Fig. 3.

The admissible passages through the meso-vertices are addressed individually taking into account the aggregated vertex structure. Since the application of *Rule C* leads to cycles in digraph G_H, this fact must be taken into account when seeking directed paths. Due to the property of a path in the graph, where no vertex must repeatedly occur, the

Algorithm 1 *(Continued).* Construction of meso-vertices in the models of rail infrastructure

```
048 function Find_C(↓G_H, ↑v_i, ↑v_j, ↑rslt)
049     rslt←none
050     foreach v_i ∈ (V(G_H) − (^T V(G_H) ∪^X V(G_H)))
051         foreach v_j ∈ (Succ(v_i) − (^T V(G_H) ∪^X V(G_H)))
052             if ((|Succ(v_i)| = 2)and(|Pred(v_j)| = 2)) then
053                 Z←(Succ(v_i)∩Pred(v_j))
054                 if |Z| = 1 then
055                     Get_Vertex(↓Z, ↑v_k)
056                     if (v_k ∉^T V(G_H)andv_i ∉ Succ(v_k)andv_k ∉ Succ(v_j)) then
057                         rslt←found
058                         exit
059                     end
060                 end
061             end
062         end
063     end
064 end
065 function Find_D(↓G_H, ↑v_i, ↑v_j, ↑rslt)
066     rslt←none
067     foreach v_i ∈^X V(G_H)
068         foreach v_j ∈ Succ(v_i)
069             if (v_j ∈ Pred(v_i)andv_j ∉ (^T V(G_H) ∪^X V(G_H))) then
070                 rslt←found
071                 exit
072             end
073         end
074     end
075 end
```

DFS algorithm will never allow any vertex to be put into the auxiliary stack more than once.

The topology of each (i-th) path found is represented by a linearly ordered set $L_i(G_H)$, i = 1,…,k, which contains those elements-vertices lying on that path. All such paths can be stored in a set $Z(G_H) = \bigcup_{i=1}^{k} L_i(G_H)$. Each of the paths found can be used in two ways in the simulator: for a simulated train run (or shunting ride) in the same direction in which the edges on the path are directed or in the opposite direction. For example, the path $[v_{25},v_1,v_3,v_5,v_7,v_{23}]$ can be traversed from v_{25} to v_{23} or from v_{23} to v_{25} (Fig. 4).

Note: The specific usability of the paths found (particularly for shunting rides) must also be assessed with respect to the train (or shunted wagons) length.

When examining the feasibility of simultaneous setting of track routes on the station throat modelled, specific unordered n-tuples $(L_1(G_H), L_2(G_H), \ldots, L_n(G_H))$, $L_i(G_H) \subset Z(G_H)$, i = 1,…,n, $2 \le n \le k$, $k = |Z(G_H)|$. N-tuples elements represent different track routes (they can be computed in *MesoINFRA* tool). If the elements/sets of a particular n-tuple meet the condition that $L_i(G_H) \cap L_j(G_H) = \emptyset$, $i \ne j$, $i,j \in \langle 1, \ldots, n \rangle$, then the routes corresponding to the n-tuple elements can be set simultaneously.

G. VERIFICATION AND VALIDATION

The target models of selected station throats and algorithms for their automated set-up (described earlier in this article) were tested within the frame of *MesoINFRA* software tool.

The testing was carried out as part of the processing of simulation-based case studies focused on the assessment of station throat capacity related to five particular Czech railway stations (Zdice, Lysá nad Labem, Cheb, Golčův Jeníkov and Prague main station).

The most extensive track station throats examined were located within the Prague Main Railway Station (Praha hl.n.). The south throat involves 47 switches and 9 track crossings (i.e., $|V(G_P) - {}^{BT}V(G_P)| = 56$) and the target hybrid mesoscopic model in its final topology (after aggregation transformations) encompassed 22 interior vertices, i.e., $|V(G_H) - {}^{BT}V(G_H)| = 22$. The north throat involves 44 switches and 1 track crossing ($|V(G_P) - {}^{BT}V(G_P)| = 45$). The target model involves 12 interior vertices, i.e., $|V(G_H) - {}^{BT}V(G_H)| = 12$. For illustration, two models of the north throat are graphically demonstrated using the outputs from *MesoINFRA* tool.

The primary/atomic model is shown in Fig. 10 and the final target hybrid model topology is presented in Fig. 11.

Algorithm 1 *(Continued).* Construction of meso-vertices in the models of rail infrastructure

```
function Aggreg_Two_Vertices(↓↑G_H, ↓v_i, ↓v_j)
    InVi ← ∅
    OutVi ← ∅
    InVj ← ∅
    OutVj ← ∅
    InVi ←(Pred(v_i)− {v_j}) // the set of predecessors of v_i (excluding v_j)
    OutVi ←(Succ(v_i)− {v_j}) // the set of successors of v_i (excluding v_j)
    InVj ←(Pred(v_j)− {v_i}) // the set of predecessors of v_j (excluding v_i)
    OutVj ←(Succ(v_j)− {v_i}) // the set of successors of v_j (excluding v_i)
    foreach v ∈ InVi
        E(G_H) ←E(G_H)− {e} // extracting input edges of v_i, φ(e) = [v,v_i]
    end
    foreach v ∈ OutVi
        E(G_H) ←E(G_H)− {e} // extracting output edges of v_i, φ(e) = [v_i,v]
    end
    foreach v ∈ InVj
        E(G_H) ←E(G_H)− {e} // extracting input edges of v_j, φ(e) = [v,v_j]
    end
    foreach v ∈ OutVj
        E(G_H) ←E(G_H)− {e} // extracting output edges of v_j, φ(e) = [v_j,v]
    end
    foreach e ∈ E(G_H)
        if ((φ(e) = [v_i, v_j])or(φ(e) = [v_j, v_i])) then
            E(G_H) ←E(G_H)− {e} // extracting edges linking vertices v_i and v_j
        end
    end
    V(G_H) ←V(G_H)− {v_i,v_j} // extracting vertices v_i,v_j
    ^M V(G_H) ←^M V(G_H)∪{u} // adding new meso-vertex u
    foreach v ∈ (OutVi ∪ OutVj)
        E(G_H) ←E(G_H)∪{e} // adding new input edges of u, φ(e) = [v,u]
    end
    foreach ⊑ ∈ (OutVi ∪ OutVj)
        E(G_H) ←E(G_H)∪{e} // adding new output edges of u, φ(e) = [u,v]
    end
end
```

TABLE 6. Auxiliary function utilized within the Algorithm 1.

Function	Specification
Get_Vertex(↓Q,↑v)	Auxiliary function accessing an element-vertex v belonging to a set Q with a specific feature: |Q| = 1

The methods of verification and validation (V&V) of simulation models are described in detail in [40]. The practical applications of these methods have been demonstrated, for example, in [38] and [39].

Considering the scope of this article, attention (with respect to V&V) was paid mainly to infrastructure sub-models and the corresponding innovative graph algorithms (forming part of the *SepSimZ* simulation tool).

From this perspective, the V&V process (concerning the infrastructure models and the algorithms that operate on them) included the following phases (as defined in [40]):

(a) Designing and forming a conceptual model
(b) Conceptual model validation
(c) Designing and building-up a computerized model
(d) Computerized model verification
(e) Operational validation of a computerized model

The experimental and verification design was based on the processing of all station throats that are parts of the five mentioned railway stations in the Czech Republic. For each station throat, an expert inspection was performed to check each transformation iteration of the corresponding digraph G_H. In addition, for each target (hybrid) infrastructure model, all meso-vertices were checked for correct feasibility of setting simultaneous train routes against the setting of simultaneous routes within the corresponding atomic model.

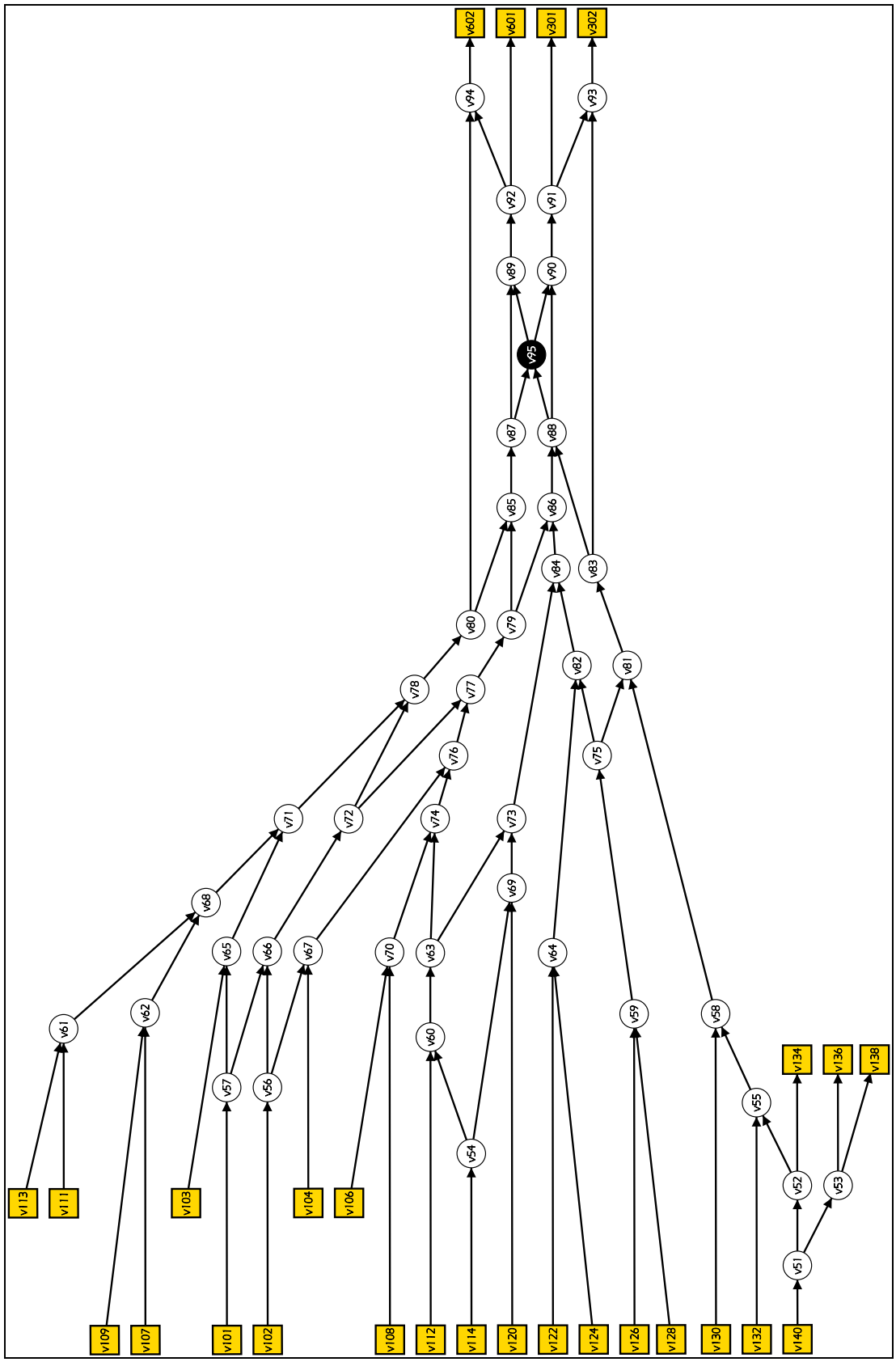

FIGURE 10. Atomic model of the north station throat (Prague main station) constructed in MesoINFRA tool.

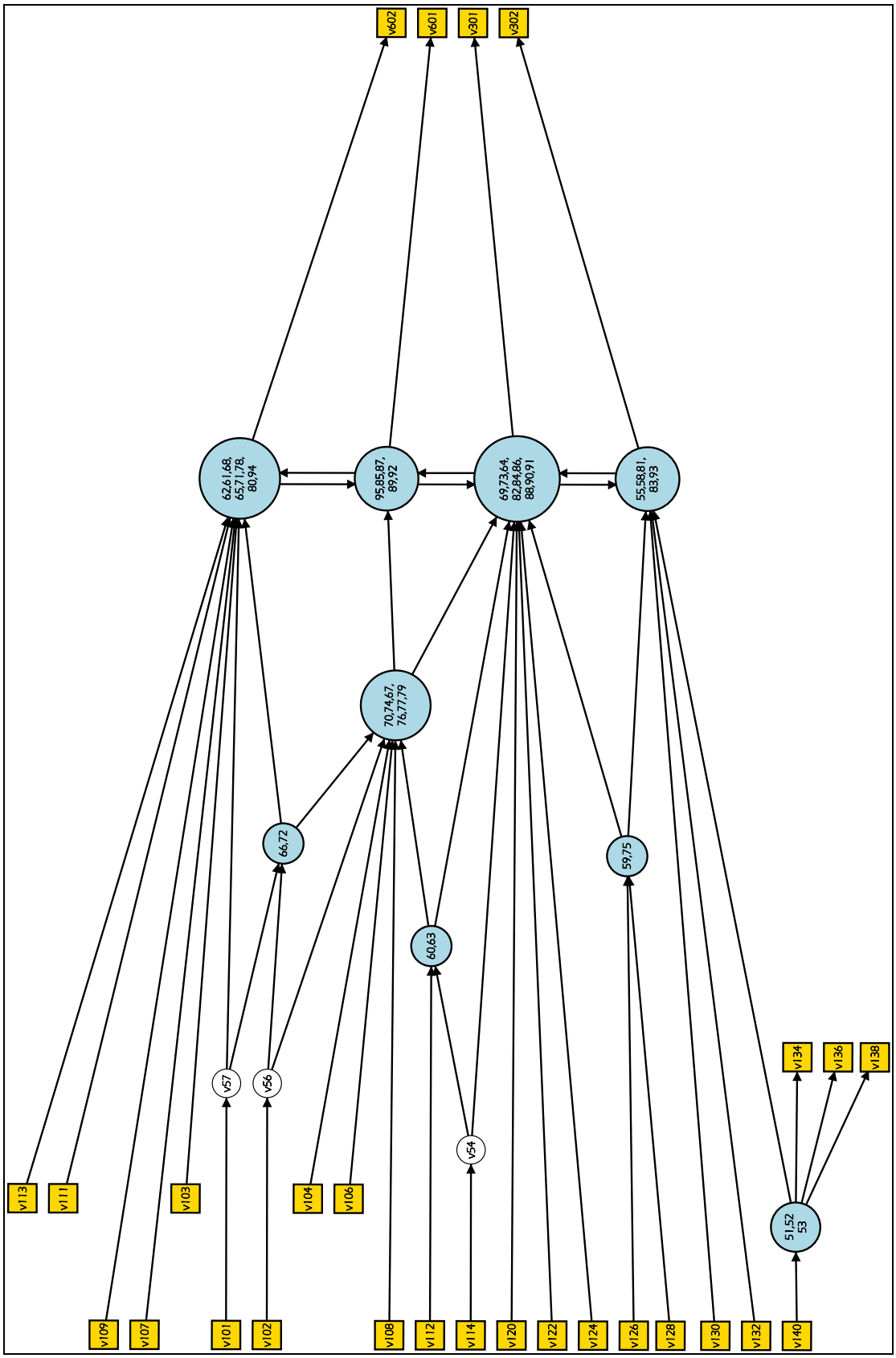

FIGURE 11. Hybrid model of the north station throat (Prague main station) computed within MesoINFRA tool.

TABLE 7. Admissible transits via atomic vertices in digraph G_H.

Vertex reflecting	Admissible transits
(*Simple*) *switch* (Fig. 3a)	$v_2 \rightarrow v_1 \rightarrow v_3$ $v_2 \rightarrow v_1 \rightarrow v_4$
Double slip switch (Fig. 3b)	$v_2 \rightarrow v_1 \rightarrow v_5$ $v_3 \rightarrow v_1 \rightarrow v_4$ $v_2 \rightarrow v_1 \rightarrow v_4$ $v_3 \rightarrow v_1 \rightarrow v_5$
Single slips switch (Fig. 3c)	$v_2 \rightarrow v_1 \rightarrow v_5$ $v_3 \rightarrow v_1 \rightarrow v_4$ $v_3 \rightarrow v_1 \rightarrow v_5$
Track crossing (Fig. 3d)	$v_2 \rightarrow v_1 \rightarrow v_5$ $v_3 \rightarrow v_1 \rightarrow v_4$
Interior sojourn track element (Fig. 3e)	$v_2 \rightarrow v_1 \rightarrow v_3$

At the (a) phase, attention was paid to the design of the conceptual model that consists of 2 parts:

- *mathematical model* (directed graph G_H) representing the topology of the station throat at the mesoscopic level of detail,
- *graph algorithms* that consecutively perform the partial transformations of the initial topology of digraph G_H.

Conceptual model validation (the phase (b)) focused on suitability assessment of the mathematical model describing the station throat topology and of selected algorithms working over the mathematical model. The *Independent Verification* and *Validation* (IV&V) approach [40], which is based on a conceptual model expert assessment by a professional in the relevant application domain, was applied. The professional was a renowned railway traffic expert who is a co-author of this paper. It was used the *Face Validation* (*Expert Validation*) method [40], which requires deep knowledge of the topic, i.e., the railway traffic system. The conceptual model validation process led to the following conclusions: (i) the devised mathematical model type for the station throat reflects sufficiently faithfully the topology of real station track throat; (ii) the algorithms for the iterative transformations of the station throat infrastructure model topology (represented by digraph G_H) are devised to create an acceptable target topology of digraph G_H (i.e., topology permitting simultaneous setting of such train routes in the simulator as faithfully reflect the options for simultaneous setting of routes on real/modelled station throat).

This was followed by setting up a *computerized model* (the phase (c)) reflecting the basic principles of the conceptual model. Implementation of this model included a suitable *memory representation* of the track model using the forward-reverse star data structure [37], [41]. This data structure enables the algorithms for digraph G_H transformations (and also algorithms for track route search) to be efficiently implemented.

Verification of this model (the phase (d)) involved a logical correctness check of the algorithm results, which were required to correspond with the applications of *Rules* $A - D$. This was made with a focus on the correctness of the digraph G_H topology after each transformation iteration. The verification exercise () was made by the authors of this paper, who found the computation results of the algorithms in the case studies logically correct. Some erroneous results were also found but they were rectified by making corrections in the algorithm implementation.

As the last phase (e), the computerized model was subjected to *operational validation*, performed (once again) by the above-mentioned railway traffic expert, again by applying the IV&V approach and using the Face Validation method. In the case studies, the operational and technical admissibility of the computerized infrastructure models for the different station throats was expertly assessed, particularly concerning the possibility of track route setting. The analysis of the models and their construction algorithms (applying the transformation *Rules* $A - D$) gave evidence that the solutions were correct/valid, both from the operational and technical aspects. The validated algorithms are part of the *MesoINFRA* tool, which is now commonly used in the process of assessing the capacity of station throats in the Czech Republic.

V. CASE STUDY

A demonstration case study was performed to illustrate the use of mesoscopic station throat infrastructure models and innovative algorithms for their construction. The study focused on the infrastructure of a prototype railway station (or the station throats). The infrastructure topology was based on the track layout of the Golčův Jeníkov railway station, located on the Czech railway network roughly 80 km southeast of the capital Prague. A segment of the schematic track layout is shown in Fig. 1.

The initial microscopic model of the infrastructure (undirected graph G_0), reflecting the schematic track layout, is shown in Figs. 2,12. The model includes (i) the WEST and EAST station throats (Fig. 12a) and (ii) station tracks ST_1–ST_4 (Fig. 12c) and line tracks LT_{NW}, LT_{SW}, LT_{NE}, LT_{SE} (Fig. 12c), which are parts of the adjacent double-track rail lines (WEST rail line and EAST rail line).

The related primary mesoscopic infrastructure model (digraph G_P) is presented in Fig. 4. The vertices of this graph (representing the models of the switches and track crossings) reflect the subgraphs from model G_0 – the graphical borders of the subgraphs are schematically shown in Fig. 12b.

The initial topology of the hybrid mesoscopic model (digraph G_H) is identical to that of the primary model G_P. The digraph G_H is then used to illustrate the iterative aggregation of the vertices (by using the procedures from *Rules* $A - D$), as commented on in section IV (Figs. 6,7). The final topology of the digraph G_H obtained after the 10^{th} transformation iteration is shown in Fig. 7.

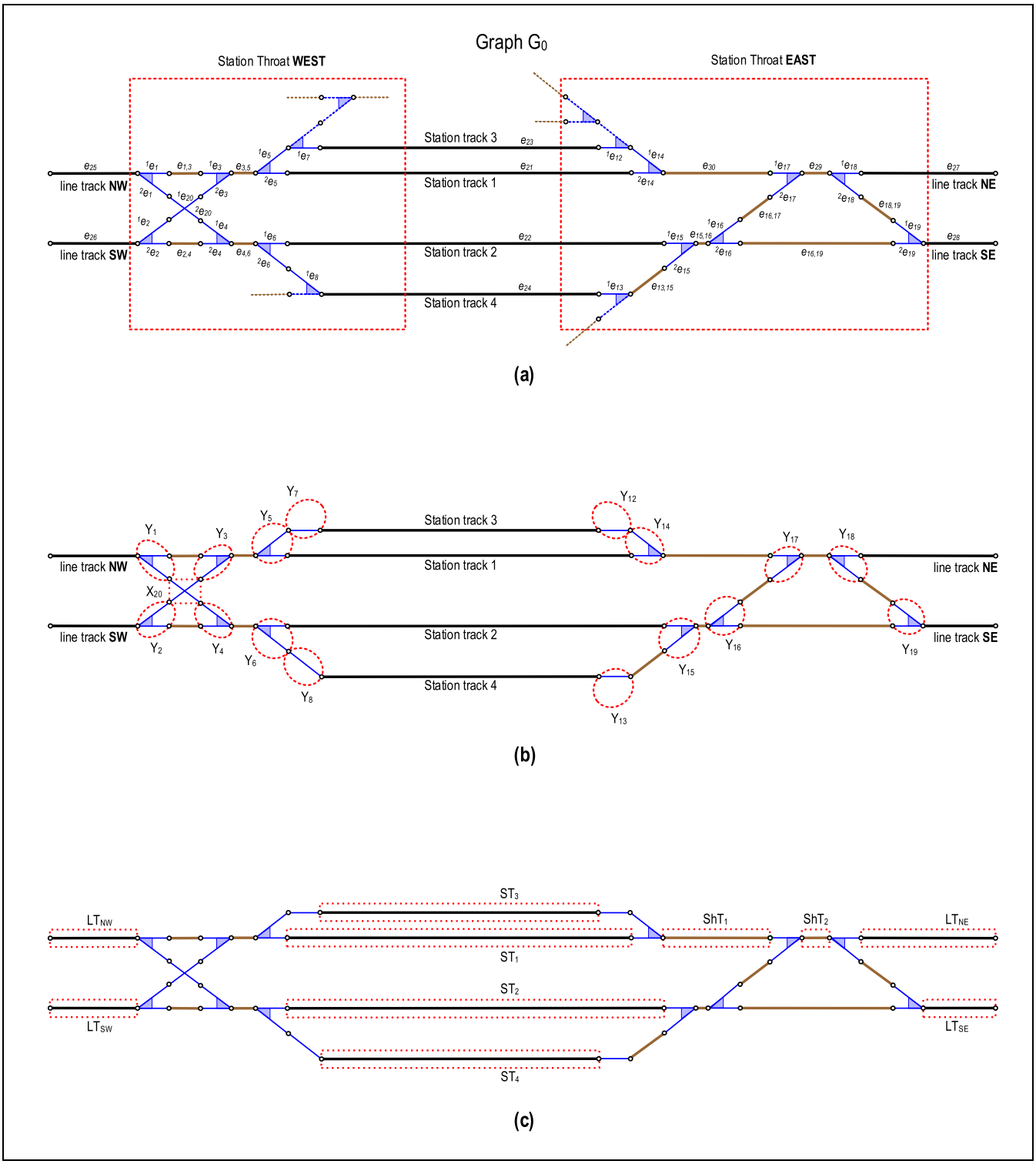

FIGURE 12. Analysis of an initial microscopic model of track infrastructure.

The separate infrastructure models of the station throats are discussed below for demonstration purposes. The specification – partial at least – of each station throat model is given below for illustration.

A. STATION THROAT WEST

The station throat WEST includes (i) 8 simple switches, (ii) 1 track crossing and (iii) 6 border sojourn track elements.

TABLE 8. Directed paths within the models reflecting station throat WEST.

Atomic paths (WEST)	Hybrid paths (WEST)
a01: [v_{25},v_1,v_3,v_5,v_{21}]	h09: [v_{25},u_{10},v_{21}]
a02: [v_{25},v_1,v_3,v_5,v_7,v_{23}]	h10: [v_{25},u_{10},v_{23}]
a03: [v_{25},v_1,v_{20},v_4,v_6,v_{22}]	h11: [v_{25},u_{10},u_9,v_{22}]
a04: [v_{25},v_1,v_{20},v_4,v_6,v_8,v_{24}]	h12: [v_{25},u_{10},u_9,v_{24}]
a05: [v_{26},v_2,v_4,v_6,v_{22}]	h13: [v_{26},u_9,v_{22}]
a06: [v_{26},v_2,v_4,v_6,v_8,v_{24}]	h14: [v_{26},u_9,v_{24}]
a07: [v_{26},v_2,v_{20},v_3,v_5,v_{21}]	h15: [v_{26},u_9,u_{10},v_{21}]
a08: [v_{26},v_2,v_{20},v_3,v_5,v_7,v_{23}]	h16: [v_{26},u_9,u_{10},v_{23}]
Simultaneous paths (pairs)	
(a01,a05) (a01,a06)	(h09,h13) (h09,h14)
(a02,a05) (a02,a06)	(h10,h13) (h10,h14)

The *microscopic model* of the station throat – the undirected graph $G_0 = (V,E,\varphi,\omega)$ – includes the following edges (Fig. 12a):

$$E_{\text{branch}}(G_0) = \{{}^1e_1, {}^2e_1, {}^1e_2, {}^2e_2, {}^1e_3, {}^2e_3, {}^1e_4, {}^2e_4, {}^1e_5, {}^2e_5, {}^1e_6, {}^2e_6, {}^1e_7, {}^1e_8\}$$
$$E_{\text{temp}}(G_0) = \{e_{21}, e_{22}, e_{23}, e_{24}, e_{25}, e_{26}\}$$
$$E_{\text{conn}}(G_0) = \{e_{1,3}, e_{2,4}, e_{3,5}, e_{4,6}\}$$

The *primary/atomic mesoscopic model* of the station throat – digraph $G_P = (V,E,\varphi,\kappa)$ – comprises the following vertices (Fig. 4):

$${}^{Y}V(G_P) = \{v_1, v_2, v_3, v_4, v_5, v_6, v_7, v_8\}$$
$${}^{X}V(G_P) = \{v_{20}\}, {}^{S}V(G_P) = \emptyset, {}^{D}V(G_P) = \emptyset, {}^{IT}V(G_P) = \emptyset$$
$${}^{T}V(G_P) = {}^{BT}V(G_P) = \{v_{21}, v_{22}, v_{23}, v_{24}, v_{25}, v_{26}\}$$

The edge direction was chosen from vertices in the set Λ ($\Lambda \subset {}^{BT}V(G_P)$) representing the track elements of the line track to vertices in the set Ω ($\Omega \subset {}^{BT}V(G_P)$) representing station tracks. The sets Λ, Ω (${}^{BT}V(G_P) = \Lambda \cup \Omega, \Lambda \cap \Omega = \emptyset$) are specified as follows:

$$\Lambda = \{v_{25}, v_{26}\}, \Omega = \{v_{21}, v_{22}, v_{23}, v_{24}\}$$

The different directed paths representing the admissible track routes on the station throat can be sought on the primary model (by using the *DFS* algorithm for instance). The topology of the directed paths can be stored in linearly ordered sets or ordered n-tuples. For each route it holds that its initial vertex is from the set Λ and the target vertex is from the set Ω.

Eight different "atomic" paths (a-paths) can be found on digraph G_P, as listed in Table 8 and shown in Figs. 13,14. Fig. 14 shows the models of the routes that cannot be set simultaneously with other routes, while Fig. 13 shows the models of admissible simultaneous routes (different colors were used for the different route models). The track routes that can be set simultaneously on the station throat are modelled by unordered pairs of directed paths, specified in Table 8 and graphically illustrated in Fig. 13.

The final topology of the *target mesoscopic hybrid station throat model* (digraph $G_H = (V,E,\varphi,\kappa)$), as obtained by 10 transformation iterations (Fig. 7), is characterized by the following vertex sets:

$${}^{Y}V(G_H) = \emptyset, {}^{X}V(G_H) = \emptyset,$$
$${}^{S}V(G_H) = \emptyset, {}^{D}V(G_H) = \emptyset, {}^{IT}V(G_H) = \emptyset$$
$${}^{T}V(G_H) = {}^{BT}V(G_H) = \{v_{21}, v_{22}, v_{23}, v_{24}, v_{25}, v_{26}\}$$
$${}^{M}V(G_H) = \{u_9, u_{10}\}$$

The edge directions and the interpretation of the Λ, Ω set elements (${}^{BT}V(G_H) = \Lambda \cup \Omega, \Lambda \cap \Omega = \emptyset$) are analogous to those of the corresponding digraph G_P. It holds for the sets Λ, Ω that:

$$\Lambda = \{v_{25}, v_{26}\}, \Omega = \{v_{21}, v_{22}, v_{23}, v_{24}\}$$

Like in digraph G_P, 8 different "hybrid" paths (h-paths) can be found in digraph G_H, as listed in Table 8 and shown in Figs. 13,14. The track routes that can be set simultaneously on the station throat are listed in Table 8 as well.

B. STATION THROAT EAST

Station throat EAST consists of (i) 8 simple switches, (ii) 2 interior sojourn track elements and (iii) 6 border sojourn track elements. Like for the station throat WEST, partial specifications of the different station throat models are given below for illustration.

The *microscopic station throat model* – undirected graph $G_0 = (V,E,\varphi,\omega)$ – contains the following edges (Fig. 12a):

$$E_{\text{branch}}(G_0) = \{{}^1e_{12}, {}^1e_{13}, {}^1e_{14}, {}^2e_{14}, {}^1e_{15}, {}^2e_{15}, {}^1e_{16}, {}^2e_{16}, {}^1e_{17}, {}^2e_{17}, {}^1e_{18}, {}^2e_{18}, {}^1e_{19}, {}^2e_{19}\}$$
$$E_{\text{temp}}(G_0) = \{e_{21}, e_{22}, e_{23}, e_{24}, e_{27}, e_{28}, e_{29}, e_{30}\}$$
$$E_{\text{conn}}(G_0) = \{e_{13,15}, e_{15,16}, e_{16,17}, e_{16,19}\}$$

The *primary/atomic mesoscopic station throat model* – digraph $G_P = (V,E,\varphi,\kappa)$ – contains the following vertices (Fig. 4):

$${}^{Y}V(G_P) = \{v_{12}, v_{13}, v_{14}, v_{15}, v_{16}, v_{17}, v_{18}, v_{19}\}$$
$${}^{X}V(G_P) = \emptyset, {}^{S}V(G_P) = \emptyset, {}^{D}V(G_P) = \emptyset$$
$${}^{BT}V(G_P) = \{v_{21}, v_{22}, v_{23}, v_{24}, v_{27}, v_{28}\},$$
$${}^{IT}V(G_P) = \{v_{29}, v_{30}\}$$

The edge direction was from the vertices in the set Λ ($\Lambda \subset {}^{BT}V(G_P)$) representing the station track elements to the vertices in the set Ω ($\Omega \subset {}^{BT}V(G_P)$) representing the line tracks. The sets Λ, Ω (${}^{BT}V(G_P) = \Lambda \cup \Omega, \Lambda \cap \Omega = \emptyset$) are specified as follows:

$$\Lambda = \{v_{21}, v_{22}, v_{23}, v_{24}\}, \Omega = \{v_{27}, v_{28}\}$$

The directed paths whose starting vertices are from the set $\Lambda^{EXT} = \Lambda \cup {}^{IT}V(G_P)$ and the target are from the set $\Omega^{EXT} = \Omega \cup {}^{IT}V(G_P)$ can be sought in the primary model. The sets are specified as follows:

$$\Lambda^{EXT} = \{v_{21}, v_{22}, v_{23}, v_{24}, v_{29}, v_{30}\},$$
$$\Omega^{EXT} = \{v_{27}, v_{28}, v_{29}, v_{30}\}$$

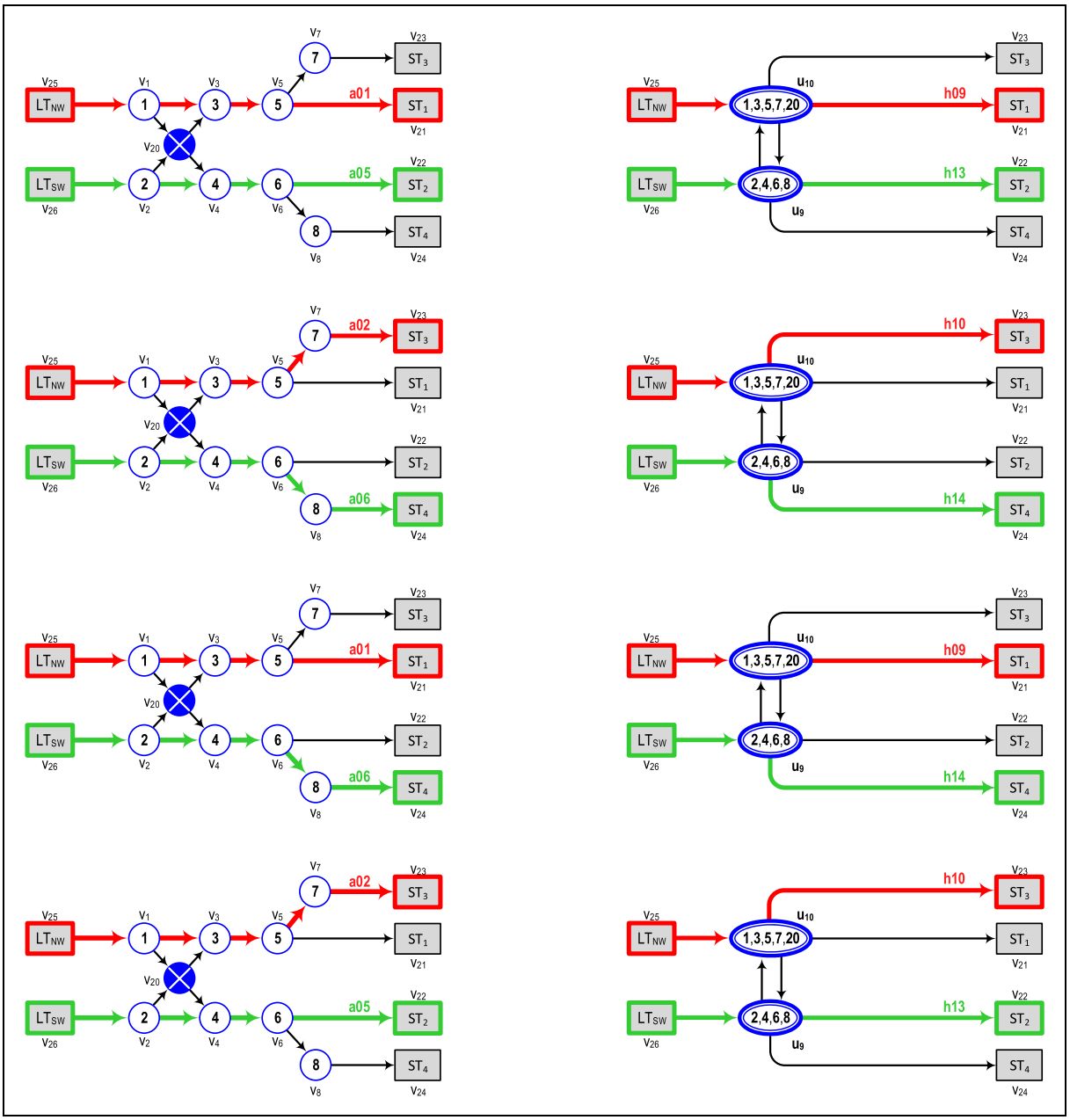

FIGURE 13. Admissible simultaneous track routes modelled by directed paths (station throat WEST).

Twenty-one different "atomic" paths (a-paths). were identified in digraph G_P(Table 9). Selected a-paths are shown in different colors in Figs. 15a,c.

Pairs and triplets of disjunct directed paths are also specified in Table 9. Selected paths of this type are shown graphically in Figs. 15a,c.

The final *target mesoscopic hybrid station throat model* topology – digraph $G_H = (V,E, \varphi, \kappa)$ – is characterized by the following vertex sets (Figs. 15b,d):

$$^{Y}V(G_H) = \{v_{17}, v_{18}, v_{19}\}, ^{X}V(G_H) = \emptyset,$$
$$^{S}V(G_H) = \emptyset ^{D}V(G_H) = \emptyset$$
$$^{BT}V(G_H) = \{v_{21},\ v_{22},\ v_{23},\ v_{24},\ v_{27}, v_{28}\},$$
$$^{IT}V(G_H) = \{v_{29}, v_{30}\}$$
$$^{M}V(G_H) = \{u_5, u_7\}$$

The edge directions and the interpretation of the set elements (members of Λ^{EXT}, Ω^{EXT}) are analogous to those in the relevant digraph G_P. The following holds for the sets Λ^{EXT}, Ω^{EXT}:

$$\Lambda^{EXT} = \{v_{21},\ v_{22},\ v_{23},\ v_{24},\ v_{29},\ v_{30}\},$$
$$\Omega^{EXT} = \{v_{27},\ v_{28},\ v_{29}, v_{30}\}$$

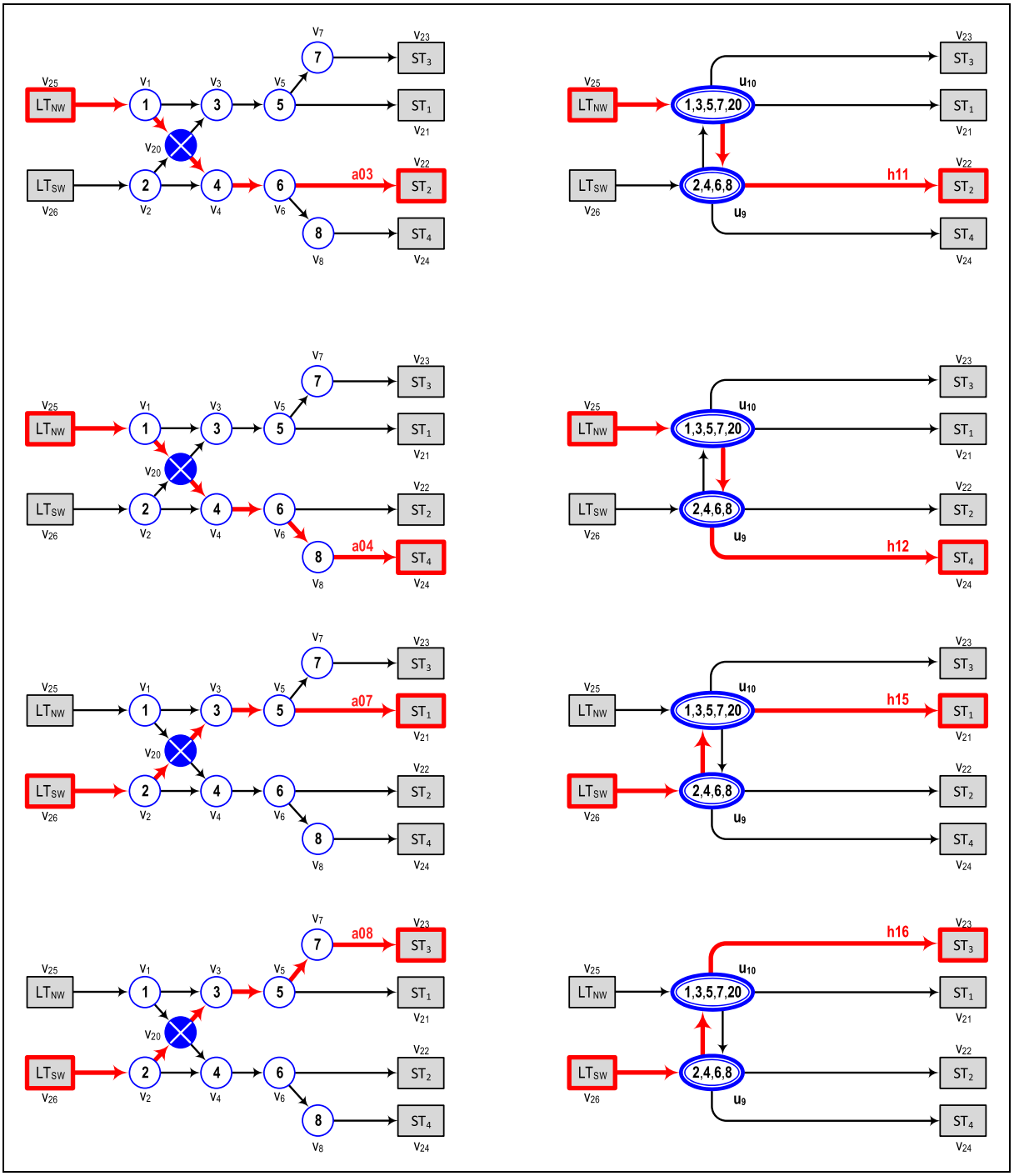

FIGURE 14. Single track routes modelled by directed paths (station throat WEST).

Like in digraph G_P, 21 different „hybrid“ paths (h-paths) can be found in digraph G_H(Table 9). Some of them are shown in Figs. 15b,d.

The unordered n-tuples of the disjunct directed paths are listed in Table 9 and some of them are shown graphically in Figs. 15b,d (the different paths are shown in different colors).

C. SEPARATE RAIL TRAFFIC SIMULATION ON STATION THROAT EAST

To illustrate the application of the *SepSim-Z* methodology, with innovative algorithms for the automated set-up of the target track infrastructure model, the case study assessed the capacity of the station throat EAST for a specific timetable. The timetable (set up by a railway traffic expert, who is also

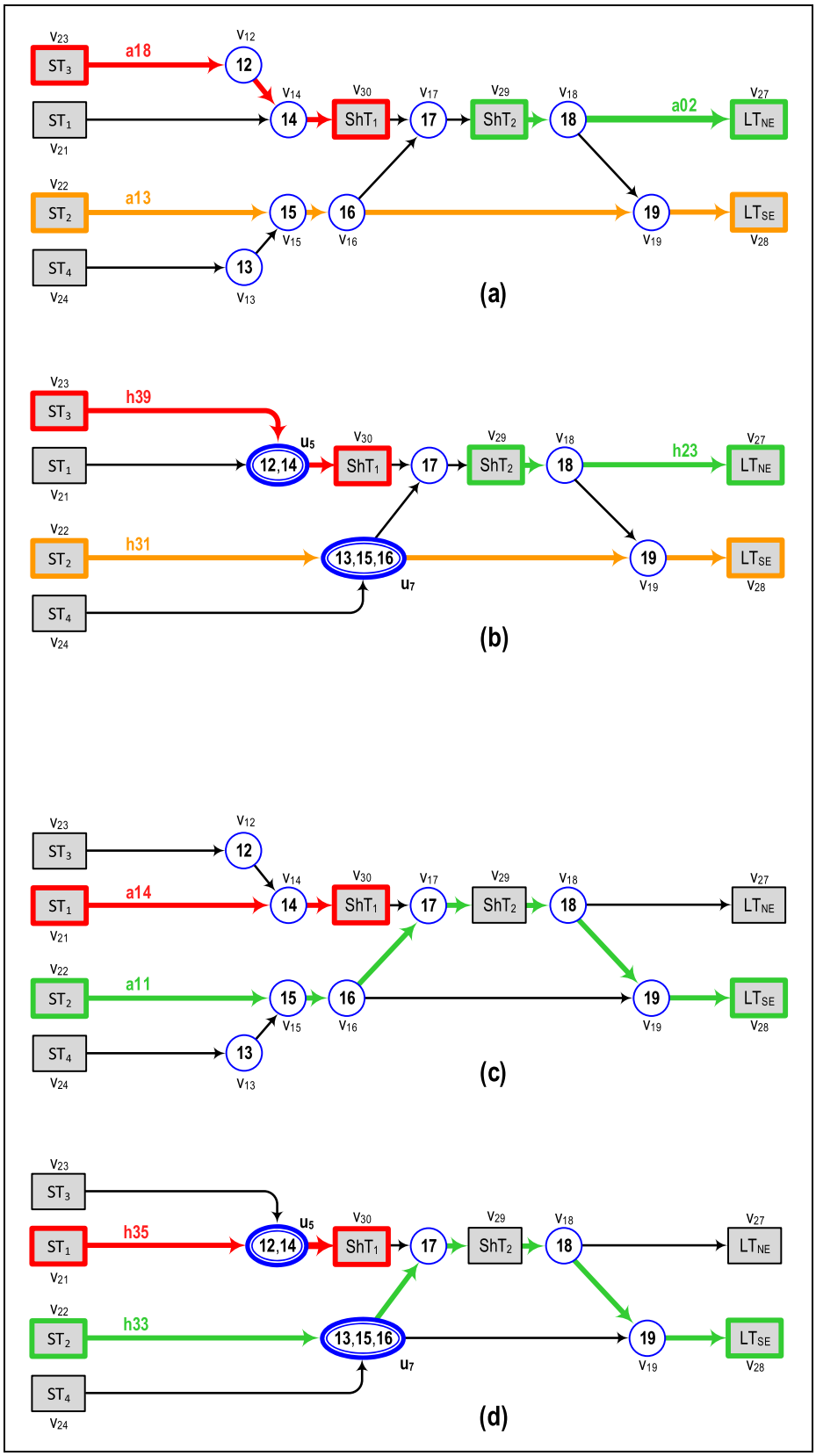

FIGURE 15. Selected simultaneous track routes modelled by directed paths (station throat EAST).

TABLE 9. Directed paths within the models reflecting station throat EAST.

Atomic paths (EAST)	Hybrid paths (EAST)
a01: [v_{29},v_{18},v_{19},v_{28}]	h22: [v_{29},v_{18},v_{19},v_{28}]
a02: [v_{29},v_{18},v_{27}]	h23: [v_{29},v_{18},v_{27}]
a03: [v_{30},v_{17},v_{29}]	h24: [v_{30},v_{17},v_{29}]
a04: [v_{30},v_{17},v_{29},v_{18},v_{19},v_{28}]	h25: [v_{30},v_{17},v_{29},v_{18},v_{19},v_{28}]
a05: [v_{30},v_{17},v_{29},v_{18},v_{27}]	h26: [v_{30},v_{17},v_{29},v_{18},v_{27}]
a06: [v_{24},v_{13},v_{15},v_{16},v_{17},v_{29}]	h27: [v_{24},u_7,v_{19},v_{28}]
a07: [v_{24},v_{13},v_{15},v_{16},v_{17},v_{29},v_{18},v_{19},v_{28}]	h28: [v_{24},u_7,v_{17},v_{29}]
a08: [v_{24},v_{13},v_{15},v_{16},v_{17},v_{29},v_{18},v_{27}]	h29: [v_{24},u_7,v_{17},v_{29},v_{18},v_{19},v_{28}]
a09: [v_{24},v_{13},v_{15},v_{16},v_{19},v_{28}]	h30: [v_{24},u_7,v_{17},v_{29},v_{18},v_{27}]
a10: [v_{22},v_{15},v_{16},v_{17},v_{29}]	h31: [v_{22},u_7,v_{19},v_{28}]
a11: [v_{22},v_{15},v_{16},v_{17},v_{29},v_{18},v_{19},v_{28}]	h32: [v_{22},u_7,v_{17},v_{29}]
a12: [v_{22},v_{15},v_{16},v_{17},v_{29},v_{18},v_{27}]	h33: [v_{22},u_7,v_{17},v_{29},v_{18},v_{19},v_{28}]
a13: [v_{22},v_{15},v_{16},v_{19},v_{28}]	h34: [v_{22},u_7,v_{17},v_{29},v_{18},v_{27}]
a14: [v_{21},v_{14},v_{30}]	h35: [v_{21},u_5,v_{30}]
a15: [v_{21},v_{14},v_{30},v_{17},v_{29}]	h36: [v_{21},u_5,v_{30},v_{17},v_{29}]
a16: [v_{21},v_{14},v_{30},v_{17},v_{29},v_{18},v_{19},v_{28}]	h37: [v_{21},u_5,v_{30},v_{17},v_{29},v_{18},v_{19},v_{28}]
a17: [v_{21},v_{14},v_{30},v_{17},v_{29},v_{18},v_{27}]	h38: [v_{21},u_5,v_{30},v_{17},v_{29},v_{18},v_{27}]
a18: [v_{23},v_{12},v_{14},v_{30}]	h39: [v_{23},u_5,v_{30}]
a19: [v_{23},v_{12},v_{14},v_{30},v_{17},v_{29}]	h40: [v_{23},u_5,v_{30},v_{17},v_{29}]
a20: [v_{23},v_{12},v_{14},v_{30},v_{17},v_{29},v_{18},v_{19},v_{28}]	h41: [v_{23},u_5,v_{30},v_{17},v_{29},v_{18},v_{19},v_{28}]
a21: [v_{23},v_{12},v_{14},v_{30},v_{17},v_{29},v_{18},v_{27}]	h42: [v_{23},u_5,v_{30},v_{17},v_{29},v_{18},v_{27}]
Simultaneous paths (pairs)	
(a01,a14) (a01,a18) (a02,a09)	(h22,h35) (h22,h39) (h23,h27)
(a02,a13) (a02,a14) (a02,a18)	(h23,h31) (h23,h35) (h23,h39)
(a03,a09) (a03,a13) (a05,a09)	(h24,h27) (h24,h31) (h26,h27)
(a05,a13) (a06,a14) (a06,a18)	(h26,h31) (h27,h35) (h27,h36)
(a07,a14) (a07,a18) (a08,a14)	(h27,h38) (h27,h39) (h27,h40)
(a08,a18) (a09,a14) (a09,a15)	(h27,h42) (h28,h35) (h28,h39)
(a09,a17) (a09,a18) (a09,a19)	(h29,h35) (h29,h39) (h30,h35)
(a09,a21) (a10,a14) (a10,a18)	(h30,h39) (h31,h35) (h31,h36)
(a11,a14) (a11,a18) (a12,a14)	(h31,h38) (h31,h39) (h31,h40)
(a12,a18) (a13,a14) (a13,a15)	(h31,h42) (h32,h35) (h32,h39)
(a13,a17) (a13,a18) (a13,a19)	(h33,h35) (h33,h39) (h34, 35)
(a13,a21)	(h34,h39)
Simultaneous paths (triplets)	
(a02,a09,a14) (a02,a09,a18)	(h23,h27,h35) (h23,h27,h39)
(a02,a13,a14) (a02,a13,a18)	(h23,h31,h35) (h23,h31,h39)

one of the authors of this paper) fits the common rail traffic intensity and composition on the main double-track railway lines in the Czech Republic.

In line with the methodological approach applied in section II, the steps of the process using the above methodology are described below.

(1) The borders of the station throat EAST were defined first on the microscopic station throat infrastructure model, represented by the undirected graph G_0 (Fig. 12a). This graph, taken from KANGO information system (which stores, among other things, information about the Czech railway infrastructure), was transferred into *MesoINFRA* tool. This tool was used to perform an automated transformation of graph G_0 to digraph G_P, which represents the primary mesoscopic infrastructure model. A diagram of this model is presented graphically in a segment of Fig. 16.

(2) Furthermore, the target mesoscopic station throat infrastructure model (based on digraph G_H), whose initial topology is identical to that of the digraph G_P, was set up automatically within *MesoINFRA*. The final topology of digraph G_H was then automatically computed by using the above-presented algorithms performing the transformation iterations according to *Rules A*−*D* (Fig. 15b,d). Digraph G_H contains meso-vertices representing groups of switches. For instance, the vertex u_7 represents (in the final digraph $G_H$topology) the group of switches that are represented by the vertices v_{13}, v_{15}, v_{16} in the digraph G_P.

(3) The runs of the trains (and the shunting rides) passing over the station throat during the relevant time period (12 a.m. – 2 p.m., i.e. 120 minutes) were identified. The runs are specified (including the train types) in the graphical timetable (Fig. 16). The timetable also includes the occupation plan for selected station tracks. So, a total of 42 train runs (including shunting rides) are examined, in 13 express train runs (shown in red), 4 regional train runs (shown in black) and 21 cargo train runs (shown in blue). The relevant time period also included 4 shunting rides of locomotives over the station throat in question (shown in green).

(4) The requisite technological times, i.e., the station headway times, which determine the minimum time spacing between each two trains passing consecutively the station throat, had not to be entered separately: they were included in the dynamically computed total times needed to relocate a train (or shunted wagons), as described below.

(5) Appropriate simulation software had to be selected and the simulation computation runs parameterization had the be performed before executing the separate mesoscopic rail traffic simulation on the station throat. One basic simulation experiment scenario (denoted *Sc01*) was specified for this study and computed in the simulation tool *SepSimZ* (see above). This scenario was associated with the following parameterization:
   - The first parameter was the station throat infrastructure model, represented by digraph G_H with its final topology. This model was taken from the *MesoINFRA* tool (Fig. 15b,d).
   - The railway traffic variant (Fig. 16) specified in step (3) constituted the next parameter.
   - The parameters for generating the random train delay occurrences (following the Bernoulli probability distribution pattern) and random delay times for each train (following the one-parametric exponential probability distribution) were set for the needs of the stochastic simulations. The generator parameter values were selected based on the recommendations in the directive *SM124* for the various train types [5], matching the real patterns of railway traffic in the Czech Republic.
   - The train priorities, affecting the assignment of the infrastructure parts to the competing applicants (trains), also play an important role in the stochastic simulations. The priority parameters of the

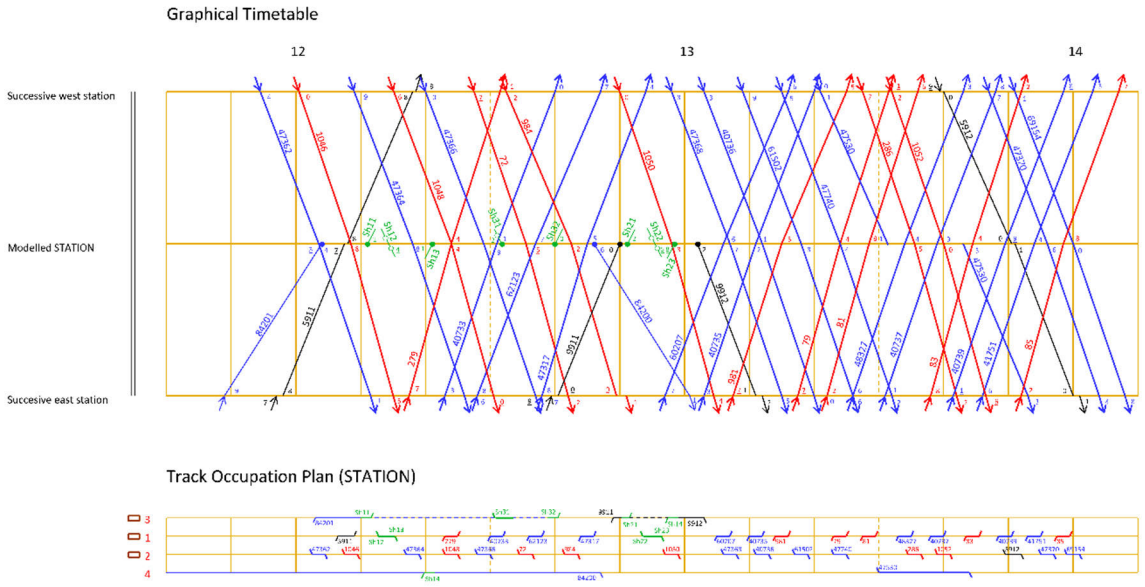

FIGURE 16. Graphical timetable.

various train types were set based on the specification in the above directive [5].

- The total times required for the relocation of a train (or shunted wagons) over parts of the station throat (represented by the relevant vertices in the hybrid digraph G_H) were obtained from the KANGO information system (see above). For each relocation, the total time includes the following parts: (i) travel time over each station throat part represented by a vertex in digraph G_H; (ii) time required to set the track route; (iii) time required to release the track route; and (iv) any additional technological time (e.g., to maintain the minimum headway – station intervals – between two train runs). The travel time is obtained by calculating the travel dynamics considering the relocation object's weight and length, the locomotive's traction characteristics, etc.
- The simulation experiment included 10,000 replications, which enable the railway traffic to be examined during the occurrence of a sufficiently high number of random effect combinations. Each replication included a 120-minute warm-up period immediately preceding the time analyzed (12 a.m. – 2 p.m.). The warm-up enabled the system to be randomly filled at the moment the period analyzed commenced.

The occurrences of conflicts on the station throat (between two trains) are predictively automatically sought during each replication run.

When a conflict is indicated a solution (taking into account the train priorities) is automatically adopted. The solution determines the order in which two trains enter the throat. For a train that will enter the throat as the second, the time position of its run is adequately shifted (with the consequence of waiting in traffic).

(6) Data, especially those concerning the train waiting times, were collected for each replication and then statistically processed, with a focus on the indicator $\bar{w}$ – *mean waiting time of trains in traffic*. Data from 10,000 replications provided the following result: $\bar{w} =$ 0.421 minutes.

(7) The station throat capacity was assessed by comparing the mean waiting time of trains in traffic $\bar{w}$ (0.421 min) obtained from the simulation with the analytically calculated limit values $\bar{w}_{opt}$ (1.065 min) and $\bar{w}_{crit}$ (1.811 min). Since $\bar{w} \leq \bar{w}_{opt}$, the station throat capacity was found sufficient for the traffic variant tested (Table 10).

TABLE 10. Capacities of station throat EAST for two scenarios of separate simulation.

Indicator	Scenario Sc01 (using digraph G_H)	Scenario Sc02 (using digraph G_P)
Sum	17.675 min	17.571 min
$\bar{w}$	0.421 min	0.418 min
Capacity	**sufficient** (with a reserve) $\bar{w} \ll \bar{w}_{opt}$	**sufficient** (with a reserve) $\bar{w} \ll \bar{w}_{opt}$
N = 42 trains Sum_{opt} = 44.750 min		
$\bar{w}_{opt}$ = 1.065 min $\bar{w}_{crit}$ = 1.811 min		

One more supplementary experiment using scenario *Sc02* was carried out to demonstrate the operational admissibility verification of the target station throat EAST infrastructure model (represented by the primary/atomic digraph G_P). The

specification of this simulation experiment differed from that using the scenario *Sc01* in the following parameters: (i) the infrastructure model used the digraph G_P (including atomic vertices only – Figs. 15a,c); (ii) the times of running over the partial station throat components are specified only for each switch and track crossing (rather than their groups modelled by meso-vertices, as used in *Sc01*). The other parameter values were identical for both scenarios.

The use of scenario *Sc02* was stimulated by the need of comparing the simulation results from scenario *Sc01* and scenario *Sc02*. It was postulated that if the results of two scenarios (mainly linked with the traffic indicator $\bar{w}$) are reasonably close, this fact can be looked upon as partial verification of the operational admissibility of the final target infrastructure model using digraph G_H. The simulation results for scenario *Sc02* are also presented in Table 10. Since the results are identical to within ± 1 %, the hybrid station throat EAST infrastructure model (which is associated with a higher degree of abstraction than the atomic model) can be considered operationally admissible.

D. COMPARATIVE ANALYSIS

In order to evaluate the simulation-based methodology *SepSim-Z* (assessing the capacities of station throats), it was compared with the commonly used analytical methodology *UIC 406* [2], which is exploited to assess the capacity of railway infrastructure both within railway lines and at railway nodes. This methodology applies the so-called *compression method*, which performs the maximum permissible elimination of the planned time spacing between pairs of trains (specified in the relevant timetable) in compliance with all current technological and technical rules of railway operation. In practice, it means that this method compresses the observed time interval of original timetable into a shorter period of time. After the compression is performed, the *occupancy time rate* (*OTR*) indicator can be calculated:

$$OTR[\%] = (OT/DTP) \times 100 \tag{4}$$

where *OT* represents the total *occupancy time* (after compression) of the throat infrastructure examined and *DTP* denotes the *defined time period* corresponding to the monitored part of the original timetable.

In order to ensure sufficient quality of railway traffic, the *UIC 406* methodology formulates a very rough proposal of what values the *OTR*-indicator should achieve. This proposal is: 60 % $\leq OTR \leq$ 80 % (Table 11).

The *OTR* indicator values were calculated for the two variants of infrastructure model (similar to the *SepSim-Z* methodology) reflecting the station throat EAST:

- hybrid mesoscopic model (represented by the target digraph G_H – a diagram of this digraph is shown in Figs. 15b,d),
- atomic mesoscopic model (represented by the primary digraph G_P – a diagram of this digraph is depicted in Figs. 15a,c).

TABLE 11. Classification of station throat capacity reflecting the occupancy time rate (OTR) indicator.

Station Throat Capacity	Value of the indicator OTR
Sufficient with a reserve	$OTR < 60$ %
Proposed	60 % $\leq OTR \leq$ 80 %
Deficient	$OTR >$ 80 %

TABLE 12. Capacities of the station throat EAST for two variants of infrastructure model *(UIC 406 methodology)*.

Indicator	Hybrid model (digraph G_H)	Atomic model (digraph G_P)
OTR	40.8 %	39.6 %
OT	49.0 min	47.5 min
Capacity	**sufficient** (with a reserve) *OTR* < 60 %	**sufficient** (with a reserve) *OTR* < 60 %
$N = 42$ trains	$DTP = 120$ min	

OTR – occupancy time rate
OT – occupancy time
DTP – defined time period

The resulting *OTR* indicator values for two mentioned models are shown in Table 12. These values differ from each other by less than 3 %, i.e., the use of the hybrid mesoscopic model can be considered operationally permissible even in the *UIC 406* methodology.

Calculations based on the utilization of the compression method were performed in the software tool *StaCap406* [19], which was developed at the University of Pardubice. A graphical illustration of the compression applied to the relevant timetable (Fig. 16) is presented in Fig. 17 (using a graphical formalism from *UIC 406*). This illustration reflects the result of a calculation that used a hybrid infrastructure model (digraph G_H).The left part of the figure shows the time positions of the trains as determined by the timetable. The right part presents the given timetable after compression.

The results from the two different methods used in the *SepSim-Z* (Table 10) and *UIC 406* (Table 12) methodologies are comparable in terms of assessing the capacity of the station throat EAST – both methods evaluated the capacity as ''sufficient (with a reserve)'' with further potential to increase the density of planned rail traffic.

Although the analytical methodology *UIC 406* is generally used for the purpose of assessing the station throat capacity (especially in European countries), its main indicator used (*OTR – occupancy time rate*) does not include in its evaluation the influence of random disturbances (train delays) that may can occur in the examined traffic. Thus, it can be stated that from a practical operational point of view, it is more appropri-

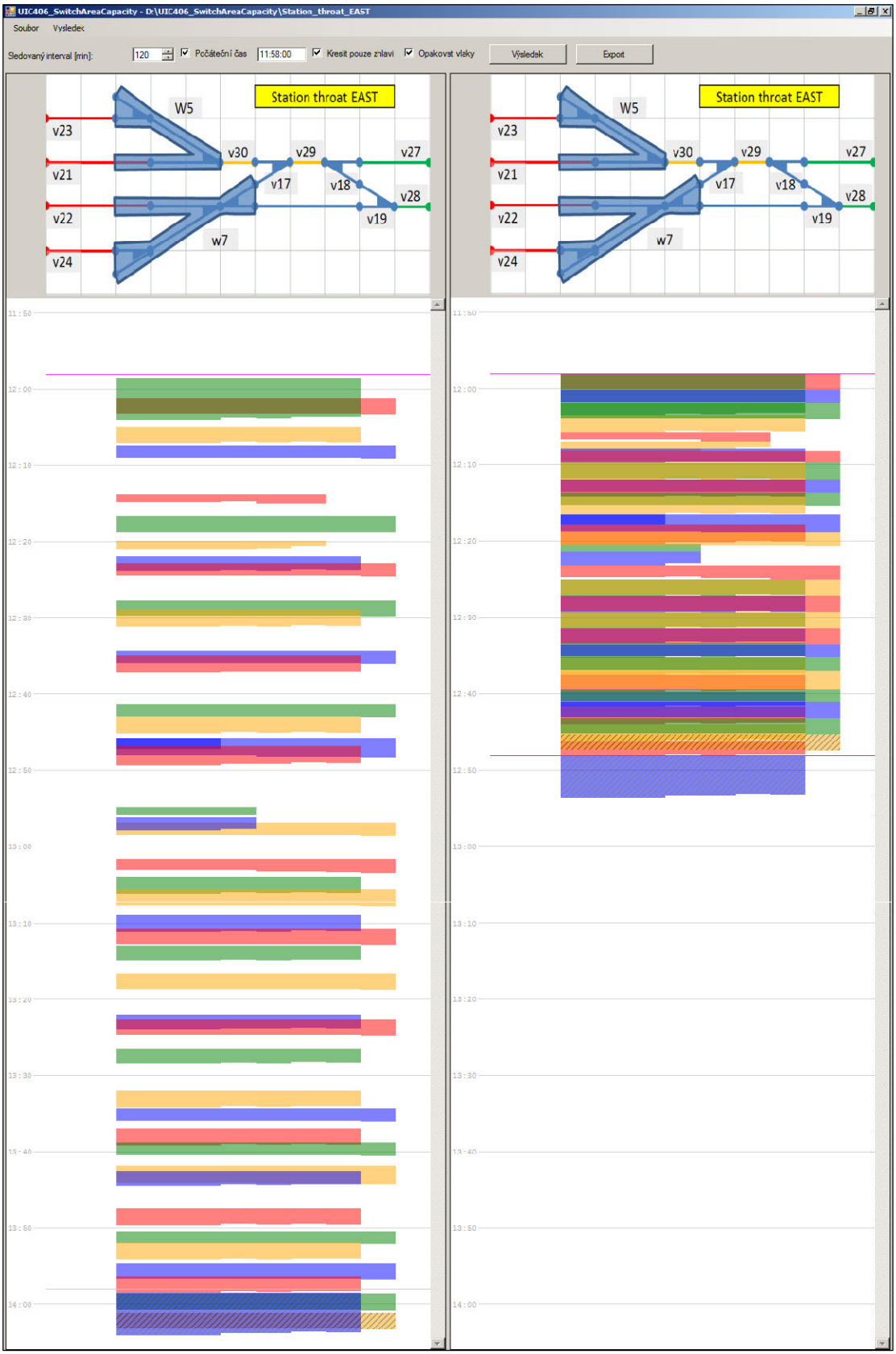

FIGURE 17. Graphical demonstration of the compression method in the StaCap406 software tool.

ate to use the *SepSim-Z* methodology (computing the traffic indicator $\bar{w}$ – *mean waiting time of trains in traffic*) for the assessment of station throats capacity, which uses computer simulation to examine the investigated traffic variant in many combinations of random train delays. It means that for experts in the field of rail transport the $\bar{w}$-indicator describes the nature of the traffic under study much more pertinently than the *OTR*-indicator.

VI. CONCLUSION

In the rail transport sector, considerable efforts are currently being devoted to improving methodologies and tools to support optimizations of rail traffic and track infrastructure. This includes the subtask of assessing the capacity of differently sized areas of rail infrastructure in relation to planned traffic volumes. Considerable attention is currently paid to station throats. The operational assessment of these track areas is very important as they typically can represent very congested locations at the junction of railway lines and railway nodes/stations and thus affect the practical throughput of the extended parts of railway networks.

Current methods of station throat capacity assessment (as presented in subsection I-B), whether they use analytical or simulation approaches, are associated with relatively laborious and time-consuming specification of input data for the relevant calculations. Therefore, there is a demand from practitioners to make appropriate innovations to existing methods in order to eliminate these problems. One of the possible ways of innovation was presented in this paper, which introduced innovative algorithms for the automated generation of the throat infrastructure models. Due to the fact (which was mentioned in subsection V-D) that simulation methodologies can assess the station throat capacity with a higher explanatory value than analytical methodologies, the choice was made to present innovative algorithms in the context of their application within the simulation-based methodology *SepSim-Z*.

A. BENETITS OF INNOVATIVE ALGORITHMS

Infrastructure models can be conveniently set up by using automated procedures, which are beneficial in that they (i) eliminate structural errors and (ii) reduce the model set-up time compared to the manual procedures. Original innovative algorithms (beneficial in both aspects) that implement the procedures for the automated set-up of a target mesoscopic station throat infrastructure model were presented in this article. The degree of abstraction in this target hybrid model is much higher than in the initial (atomic) model, owing to which its parameterization in the simulators is appreciably simpler (and less time-consuming) than for the more complex models. Despite its higher degree of abstraction, this model can be regarded as operationally admissible because it faithfully reflects the options for setting both single and simultaneous track routes on the station throat.

The deployment of the innovative algorithms helped to enhance the *SepSim-Z* methodology, which is used to assess the station throat capacities in the Czech Republic. This methodology is based on principles that are generally valid within any railway system, i.e., it also has good potential for use in other countries. The usability of the algorithms is, of course, much wider, potentially also in the construction of infrastructure models for differently aimed simulators (e.g., *MesoRail* [34]) or analytical methods (e.g., *UIC 406* [2]).

B. PERSPECTIVES FOR FURTHER DEVELOPMENT

Prospects for further development in the field of methods for evaluating station throat capacity lie in the development of further innovations related to better software support for inputting characteristics of train rides taking into account the technical and technological rules applicable in rail transport. It is assumed that this support should be based on a pre-built base of predefined datasets reflecting the relevant characteristics of different train types (e.g., train lengths, train weights, ride time characteristics reflecting train dynamics, etc.). For the user of the respective software tool, this would mean that he would enter the input parameters by making selections from already pre-built alternatives – this would greatly reduce the laboriousness of building the target model.

The above approach should contribute to further rationalisation (and further time saving) of data entry to ensure correct modelling of train movements on the throat infrastructure under investigation.

REFERENCES

[1] N. Niessen, "Waiting and loss probabilities for route nodes," in *Proc. 5th Int. Seminar Railway Oper. Modeling Anal.*, Copenhagen, Denmark, 2013, pp. 1–17. [Online]. Available: https://www.via.rwth-aachen.de/downloads/Niessen_Waiting%20and%20loss%20probabilities%20for%20route%20nodes.pdf

[2] *UIC Code 406—Capacity*, International Union of Railways, France, Paris, 2013.

[3] D. Janecek and F. Weymann, "LUKS-analysis of lines and junctions," in *Proc. 12th World Conf. Transp. Res. (WCTR)*, 2010, pp. 1–15.

[4] S. Han, Y. Yue, and L. Zhou, "Carrying capacity of railway station by microscopic simulation method," in *Proc. 17th Int. IEEE Conf. Intell. Transp. Syst. (ITSC)*, Oct. 2014, pp. 2725–2731, doi: 10.1109/ITSC.2014.6958126.

[5] *Directive SM124—Railway Capacity Assessment*, Rail Infrastructure Administration, Prague, Czech Republic, 2019.

[6] N. Bešinovic and R. M. P. Goverde, "Capacity assessment in railway networks," in *Handbook of Optimization in the Railway Industry*. Cham, Switzerland: Springer, 2018, pp. 25–45, doi: 10.1007/978-3-319-72153-8_2.

[7] A. Radtke and D. Hauptmann, "Automated planning of timetables in large railway networks using a microscopic data basis and railway simulation techniques," *WIT Trans. Built Environ.*, vol. 10, p. 74, May 2004.

[8] L. W. Jensen, A. Landex, O. A. Nielsen, L. G. Kroon, and M. Schmidt, "Strategic assessment of capacity consumption in railway networks: Framework and model," *Transp. Res. C, Emerg. Technol.*, vol. 74, pp. 126–149, Jan. 2017, doi: 10.1016/j.trc.2016.10.013.

[9] R. Francesco, M. Gabriele, and R. Stefano, "Complex railway systems: Capacity and utilisation of interconnected networks," *Eur. Transp. Res. Rev.*, vol. 8, no. 4, pp. 1–10, 2016, doi: 10.1007/s12544-016-0216-6.

[10] A. Kianinejadoshah and S. Ricci, "Capacity assessment in freight-passengers complex railway nodes: Trieste case study," *Infrastructure*, vol. 7, no. 8, pp. 1–12, 2022.

[11] R. Wang, L. Nie, and Y. Tan, "Evaluating line capacity with an analytical UIC code 406 compression method and blocking time stairway," *Energies*, vol. 13, no. 7, p. 1853, Apr. 2020, doi: 10.3390/en13071853.

[12] J. Armstrong and J. Preston, "Capacity utilisation and performance at railway stations," *J. Rail Transp. Planning Manage.*, vol. 7, no. 3, pp. 187–205, Dec. 2017, doi: 10.1016/j.jrtpm.2017.08.003.

[13] N. Nießen, "Leistungskenngrößen für gesamtfahrstraßenknoten," Ph.D. thesis, Verkehrswissenschaftliches Institut der Rhein, Aachen, Germany, 2016. [Online]. Available: https://core.ac.uk/download/pdf/36417197.pdf

[14] L. Liu, L. Gan, and H. Guo, "Integrated calculation of the throat in railway stations," in *Proc. ICTE*, 2011, pp. 925–930, doi: 10.1061/41184(419)153.

[15] M. Abril, F. Barber, L. Ingolotti, M. A. Salido, P. Tormos, and A. Lova, "An assessment of railway capacity," *Transp. Res. E, Logistics Transp. Rev.*, vol. 44, no. 5, pp. 774–806, 2008, doi: 10.1016/j.tre.2007.04.001.

[16] A. Landex, B. Schittenhelm, A. H. Kaas, and J. Schneider-Tilli, "Capacity measurement with the UIC 406 capacity method," in *Proc. WIT Trans. Built Environ.*, Aug. 2008, pp. 55–64, doi: 10.2495/CR080061.

[17] T. Lindner, "Applicability of the analytical UIC code 406 compression method for evaluating line and station capacity," *J. Rail Transp. Planning Manage.*, vol. 1, no. 1, pp. 49–57, Nov. 2011, doi: 10.1016/j.jrtpm.2011.09.002.

[18] I. Johansson and N. Weik, "Strategic assessment of railway station capacity—Further development of a UIC 406-based approach considering timetable uncertainty," in *Proc. 9th Int. Conf. Railway Oper. Modelling Anal.*, Beijing, China, Nov. 2021, pp. 3–7. [Online]. Available: https://www.diva-portal.org/smash/get/diva2:1619837/FULLTEXT01.pdf

[19] A. Kavička, R. Diviš, and P. Veselý, "Railway station capacity assessment utilizing simulation-based techniques and the UIC406 method," in *Proc. 32nd Eur. Modeling Simulation Symp. (EMSS)*, 2020, pp. 41–49, doi: 10.46354/i3m.2020.emss.007.

[20] W. Schwanhäußer, "Die bemessung der pufferzeiten im fahrplangefüge der eisenbahn," Ph.D. thesis, Verkehrswissenschaftliches Institut der Rheinisch-Westfälischen Technischen Hochschule, Aachen, Germany, 1974. [Online]. Available: https://www.via.rwth-aachen.de/downloads/Dissertation_Schwanhaeusser_2te_Auflage_Text.pdf

[21] W. Schwanhäußer, "Wirtschaftlich und betrieblich optimale zugzahlen auf eisenbahnstrecken," in *Eisenbahntechnische Rundschau (ETR)*. Hamburg, Germany: Eurailpress, 2009, pp. 488–495.

[22] D. B. Netz, "Richtlinie 405 fahrwegkapazität," DB Netz, Frankfurt, Germany, Tech. Rep. 2008/405, 2009.

[23] R. Prinz, B. Sewczyk, and M. Kettner, "NEMO. Netz—Evaluationsmodell bei der ÖBB," in *Eisenbahntechnische Rundschau (ETR)*, vol. 50, no. 3. Hamburg, Germany: Eurailpress, 2001, pp. 117–121.

[24] H.-J. Lim, "A model and evaluation of route optimization in nested NEMO environment," *IEICE Trans. Commun.*, vol. 88, no. 7, pp. 2765–2776, Jul. 2005, doi: 10.1093/ietcom/e88-b.7.2765.

[25] L. W. Jensen, O. A. Nielsen, and A. Landex, "Robustness indicators and capacity models for railway networks," Tech. Univ. Denmark, Lyngby, Denmark, Tech. Rep. 127799736, 2015.

[26] N. Adamko and V. Klima, "Optimisation of railway terminal design and operations using Villon generic simulation model," *Transport*, vol. 23, no. 4, pp. 335–340, Dec. 2008, doi: 10.3846/1648-4142.2008.23.335-340.

[27] M. H. F. Aly, H. Hemeda, and M. A. El-Sayed, "Computer applications in railway operation," *Alexandria Eng. J.*, vol. 55, no. 2, pp. 1573–1580, Jun. 2016, doi: 10.1016/j.aej.2015.12.028.

[28] F. Nunez, F. Reyes, P. Grube, and A. Cipriano, "Simulating railway and metropolitan rail networks: From planning to on-line control," *IEEE Intell. Transp. Syst. Mag.*, vol. 2, no. 4, pp. 18–30, Apr. 2010, doi: 10.1109/MITS.2010.939923.

[29] Y. Cui, U. Martin, and J. Liang, "PULSim: User-based adaptable simulation tool for railway planning and operations," *J. Adv. Transp.*, vol. 2018, pp. 1–11, Jan. 2018, doi: 10.1155/2018/7284815.

[30] A. Sajedinejad, S. Mardani, E. Hasannayebi, S. A. R. M. Mohammadi, and A. Kabirian, "SIMARAIL: Simulation based optimization software for scheduling railway network," in *Proc. Winter Simulation Conf. (WSC)*, Dec. 2011, pp. 3730–3741, doi: 10.1109/WSC.2011.6148066.

[31] M. Zhong, Y. Yue, and D. Li, "Analyzing and evaluating infrastructure capacity of railway passenger station by mesoscopic simulation method," in *Proc. Int. Conf. Intell. Rail Transp. (ICIRT)*, Dec. 2018, pp. 1–5, doi: 10.1109/ICIRT.2018.8641593.

[32] S. Saidi, N. H. M. Wilson, H. N. Koutsopoulos, and J. Zhao, "Mesoscopic modeling of train operations: Application to the MBTA red line," in *Proc. IEEE Intell. Transp. Syst. Conf. (ITSC)*, Oct. 2019, pp. 98–103, doi: 10.1109/ITSC.2019.8917313.

[33] M. Marinov and J. Viegas, "A mesoscopic simulation modelling methodology for analyzing and evaluating freight train operations in a rail network," *Simul. Model. Pract. Theory*, vol. 19, no. 1, pp. 516–539, 2011, doi: 10.1016/j.simpat.2010.08.009.

[34] R. Diviš and A. Kavička, "Reflective nested simulations supporting optimizations within sequential railway traffic simulators," *ACM Trans. Model. Comput. Simul.*, vol. 32, no. 1, pp. 1–34, Jan. 2022, doi: 10.1145/3467965.

[35] L. Fiala, "Proposal of a methodology focused on constructing aggregated elements of station throats models," in *Proc. Sci. Czech Railways*, 2013, pp. 1–11.

[36] K. Pavel, "New methodology of railway capacity assessment," in *Proc. Sci. Railway Infrastruct. Admin.*, 2020, pp. 112–130.

[37] G. R. Waissi, *Network Flows: Theory, Algorithms, and Applications*. Essex, U.K.: Prentice-Hall, 2014.

[38] A. Kavicka and R. Divis, "Dynamic search of train shortest routes within microscopic traffic simulators," *IEEE Access*, vol. 10, pp. 90163–90199, 2022, doi: 10.1109/ACCESS.2022.3197660.

[39] A. Kavicka and P. Krýže, "Dynamic automated search of shunting routes within mesoscopic rail-traffic simulators," *J. Adv. Transp.*, vol. 2021, pp. 1–22, Apr. 2021, doi: 10.1155/2021/8840516.

[40] R. G. Sargent, "Verification and validation of simulation models," in *Proc. Winter Simulation Conf.*, Dec. 2010, pp. 166–183, doi: 10.1109/WSC.2010.5679166.

[41] J. Ebert, "A versatile data structure for edge-oriented graph algorithms," *Commun. ACM*, vol. 30, no. 6, pp. 513–519, Jun. 1987, doi: 10.1145/214762.214769.

PETR VESELÝ was born in Olomouc, in 1971. He received the Master of Science degree in engineering from the University of Žilina, Slovakia, in 1994. Since 1998, he has been with the University of Pardubice, Czech Republic, where he is currently an Assistant Professor with the Faculty of Electrical Engineering and Informatics.

ANTONÍN KAVIČKA was born in Prostějov, in 1965. He received the Master of Science degree in engineering from the University of Transport and Communications, Žilina, Czechoslovakia, in 1989, and the Ph.D. degree in automatic control from the University of Žilina, Slovakia, in 1998. Since 2002, he has been with the University of Pardubice, Czech Republic, where he is currently a Full Professor and the Head of the Department of Software Technologies, Faculty of Electrical Engineering and Informatics.

PAVEL KRÝŽE was born in Liberec, in 1976. He received the Master of Science degree in engineering and the Ph.D. degree from the University of Pardubice, Czech Republic, in 1999 and 2005, respectively. He is currently with the Czech State Company Railway Infrastructure Administration (the main railway infrastructure operator in the Czech Republic), where he deals with railway infrastructure capacity issues.